Nonlinear Equilibrium and Perturbation Solutions for a Hose-Drogue Aerial Refueling System

by

Diane Vivian DeWalt

Thesis submitted to the Faculty of the

Virginia Polytechnic Institute and State University

in partial fulfillment of the requirements for the degree of

Master of Science

in

Aerospace Engineering

APPROVED:

Dr. H. L. Stalford, Chairman

Dr. E. M. Cliff

Dr. J. A. Burns

November, 1987

Blacksburg, Virginia

Nonlinear Equilibrium and Perturbation Solutions for a

Hose-Drogue Aerial Refueling System

by

Diane Vivian DeWalt

Dr. H. L. Stalford, Chairman

Aerospace Engineering

(ABSTRACT)

Several mathematical models are developed for a hose-drogue refueling system in an attempt to represent the physical system accurately and to subsequently observe the dynamic response of the system under different initial conditions. The mathematical models examined include a flexible hose model and a model which includes elastic bending effects. The equations of motion include aerodynamic, gravitational, and tensile forces, and solutions of the refueling system are found using fewer assumptions than in previous work.

Once the equations of motion are developed, they are separated into equilibrium and perturbation portions. Solutions of the nonlinear equilibrium tension distribution are obtained by solving the equations in closed form using a two point boundary value problem solver program. The solution to the linear equilibrium tension distribution is found and compared to the nonlinear

solutions. Results indicate that the behavior of the solutions is similar, but the linear solution gives larger values of tension near the hose attachment point.

The perturbation equation is discretized using a finite difference scheme and the resulting first order differential matrix equation is integrated to calculate the dynamic response for given parameters and initial conditions with the various equilibrium tension distribution solutions. Results show negligible differences between the different tension values upon substitution and it is therefore recommended that the linear aprroximation to the equilibrium tension distribution be used in analysis of this hose-drogue refueling system because of the ease in obtaining solutions with this method.

Acknowledgments

I wish to thank my committee chairman, Dr. Harold L. Stalford, for persuading me to pursue a Master's degree and for his guidance in helping me to accomplish my goals. I am also very grateful to Dr. John A. Burns and Dr. Eugene M. Cliff for their advice, support, and wisdom throughout the year. It has been a pleasure to work with them.

I am deeply indebted to my parents, Gary and Eleanor DeWalt, whose love, thoughtfulness, and continued encouragement have enabled me to achieve far more than I believed was possible. Many thanks are given to my good friends. They always made the time to help me whenever I needed it.

This thesis is dedicated to my son Nathan for he is what makes all my efforts worthwhile.

Table of Contents

List of Tables

List of Figures

Nomenclature

C_D	Hose Drag Coefficient
C_F	Hose Coefficient of Friction
D_D	Drogue Drag
EI	Hose Bending Stiffness
g	Gravitational Constant
h	Step in Space
L	Hose Length
R	Hose Radius
T	Tension
$\overline{T}$	Equilibrium Tension
U	Tow Velocity
W_D	Drogue Weight

Greek:

α	Hose Angle of Attack
ε	Local Axial Coordinate
ρ	Air Density
$\tilde{\rho}$	Linear Hose Density
ζ	Local Transverse Coordinate

Chapter 1. Introduction

In these days of advanced technology many nations rely heavily on their aircraft as a means of transportation and for defense purposes. A nation's air force performs many valuable duties, including cargo transport, reconnaissance missions, and missions involving fighter aircraft. Often these missions must be carried out over long distances beyond the normal range of an aircraft. Inflight refueling provides an air force with a larger range of possible missions and a more economical and effective means of completing them.

1.1 REFUELING METHODS

The capability of refueling an aircraft during flight has proven to be essential in the design of advanced fighters. Currently there are over 8100 aircraft equipped with inflight refueling devices in the United States alone [ref. 1]. Two

types of inflight aircraft refueling systems are in operation today; the boom refueling system and the hose-drogue refueling system.

1.1.1 Boom Refueling System

The boom refueling system acheives refueling by placing a refueling apparatus, called a boom, on the underside of a tanker aircraft, typically a KC-135 tanker. The boom is a rigid member which encases the refueling hose. It has airfoils attached to its free end which provide a boom operator, lying in the belly of the aircraft, with a means to control the position of the boom. A receiver aircraft flying behind the tanker must maintain a steady position so that the boom operator can extend the hose through the end of the boom into the receiver's receptacle and thus lock on and begin pumping fuel. Note that both aircraft must remain in a steady position relative to one another while the boom is flown into position.

1.1.2 Hose-Drogue Refueling System

The hose-drogue system is an entirely different refueling method in that the refueling hose no longer has a rigid casing and it is not controlled by any means. This hose is flexible and is constructed of several layers including rubber, wire braid, tape wrap, and other materials [fig. 1]. It collapses when empty and is wound up on a reel, much like a garden hose, and this reel mechanism is attached to the main spars in the fuselage of the tanker [fig. 2].

Attached to the free end of the flexible hose is a basket-like device called a drogue [fig. 3]. The drogue acts as a receptacle for the refueling process and also provides aerodynamic forces at the end of the hose to help it attain a nearly horizontal position during flight. The receiver aircraft must now be equipped with a device called a probe which can be inserted into the drogue and locked into position at which time the refueling process can begin. Note that it is now the responsibility of the receiver aircraft to maneuver into position while the refueling hose is free to move about in the atmosphere without control.

1.2 RESEARCH OBJECTIVES

The hose-drogue refueling system will be the subject of this research. In particular, the equations of motion of the refueling hose will be developed for the time after the hose is deployed but before attachment has taken place. It is necessary to analyze this portion of the refueling process because of the problems that are associated with an uncontrolled flexible hose. An atmospheric disturbance acting on this type of refueling system, such as a gust of wind, may cause oscillations in the hose which can grow under the proper conditions and jeopardize the refueling process.

The objectives of this thesis are

- To construct a mathematical model which accurately describes the behavior of the physical system.
- To obtain solutions to the nonlinear equilibrium equations using a two point boundary value problem solver which uses a multiple shooting method.
- To run simulations of the perturbation equations and observe the dynamic behavior of the hose under different initial conditions.

To construct any mathematical model of the hose which is useful, it is necessary to make many assumptions along the way. The choice of these assumptions is left to the researcher and often assumptions are made to simplify a problem when they may not be justifiable. This paper will use fewer assumptions than previous research of the same nature, and in particular will solve the nonlinear form of the equilibrium tension distribution and compare it to the previous solutions obtained from the linearized form of the same equation.

Chapter 2. Development of the Nonlinear Equations of Motion

The basis for the development and derivation of the equations of motion in chapter two are based on reports published by AERCOL, an aerospace consulting company which did research sponsored by the U S Air Force [ref 2, 3]. It has been the major source of information used throughout this research paper. A majority of the equations in this chapter come from this reference, with corrections and changes made where appropriate.

The equations of motion are developed for the refueling hose while it is in its extended position and allowed to hang freely in the atmosphere. The effect of the drogue attached to the free end of the hose is accounted for in the boundary conditions applied to that end. The forces acting on the hose include aerodynamic, gravitational, and tensile forces. These forces are

summed over a hose element of length ds, where s is the position coordinate along the hose, to produce the general hose equation of motion in two dimensions. For simplicity a local coordinate system is used where ε is the axial coordinate which runs along the length of the hose in its steady state position (neglecting any curvature), and ζ is the transverse coordinate which is perpendicular to the hose [fig 4]. Now the equation of motion can be written in the local coordinate system as

$$(\vec{F}_a + \vec{F}_g + \vec{F}_T = \tilde{\rho} ds \ddot{\varepsilon}) \vec{b}_1 \tag{2.1}$$

$$(\vec{F}_a + \vec{F}_g + \vec{F}_T = \tilde{\rho} ds \ddot{\zeta}) \vec{b}_2 \tag{2.2}$$

It is assumed that the hose remains coincident with the ε axis in its equilibrium state and that any deflections from this straight line are small. Physically it is known that the hose will curve slightly towards the free end because of the drag force acting on the hose and drogue. Motion will occur in the transverse direction only and axial vibrations will be neglected. The variable s can now be replaced by the variable ε in the equations since they are approximately equal.

2.1 AERODYNAMIC FORCES

The expression used for the aerodynamic forces acting on the hose is based on tests conducted by the Air Force on the hose during flight. This force is split up into components normal and tangential to the hose. The component of the aerodynamic force normal to a segment of the hose is given by

$$F_N = \rho R(U + u')^2\{C_D \sin^2(\alpha + \frac{\partial \zeta}{\partial \varepsilon})\} \tag{2.3}$$

$$+ \rho R(U + u')^2\{C_F[1 + \sin(\alpha + \frac{\partial \zeta}{\partial \varepsilon})] \sin(\alpha + \frac{\partial \zeta}{\partial \varepsilon})\}$$

The expression for the force tangential to the hose is

$$F_T = U^2 \rho R C_F[1 + \sin(\alpha + \frac{\partial \zeta}{\partial \varepsilon})] \cos(\alpha + \frac{\partial \zeta}{\partial \varepsilon}) \tag{2.4}$$

The total angle of attack in these equations has been written as

$$\alpha + \frac{\partial \zeta}{\partial \varepsilon} \tag{2.5}$$

where α represents the angle of attack at the attachment point of the hose in its equilibrium position. Equivalently this is the angle measured from a local

horizontal line, drawn under the tanker aircraft, to the ε axis. $\frac{\partial \zeta}{\partial \varepsilon}$ represents the change in angle of attack along the hose. It is assumed that the variable ζ consists of an equilibrium portion $\hat{\zeta}$ and a perturbation portion ζ'

$$\zeta = \hat{\zeta} + \zeta' \tag{2.6}$$

It is assumed that the change in angle of attack is very small for both the equilibrium and perturbation terms.

$$\frac{\partial \hat{\zeta}}{\partial \varepsilon} << 1 \tag{2.7}$$

$$\frac{\partial \zeta'}{\partial \varepsilon} << 1 \tag{2.8}$$

The following assumption has also been made

$$u' \sin \alpha = \frac{\partial \zeta'}{\partial t} \tag{2.9}$$

where the quantity u' represents a small deviation in speed from the tow speed U. Small angle assumptions have also been made when expanding the trigonometric terms.

After incorporating the simplifying assumptions and expanding terms, the equations can now be written as

$$F_N = U\rho R\{[2U(C_D + C_F)\sin\alpha\cos\alpha + UC_F\cos\alpha]\frac{\partial\hat{\zeta}}{\partial\varepsilon}\} + \tag{2.10}$$

$$U\rho R\{U[2(C_D + C_F)\sin\alpha\cos\alpha + C_F\cos\alpha]\frac{\partial\zeta'}{\partial t}\} +$$

$$U\rho R\{U(C_D + C_F)\sin^2\alpha + C_F U\sin\alpha\} +$$

$$U\rho R\{[2(C_D + C_F)\sin\alpha + 2C_F]\frac{\partial\zeta'}{\partial t}\}$$

$$F_T = \rho U^2 R C_F\{(1 + \sin\alpha)\cos\alpha + (\cos^2\alpha - \sin^2\alpha - \sin\alpha)\frac{\partial\hat{\zeta}}{\partial\varepsilon}\} \tag{2.11}$$

The aerodynamic force written in vector notation is

$$\vec{F}_a = F_T\vec{b}_1 + F_N\vec{b}_2 \tag{2.11}$$

2.2 GRAVITATIONAL FORCES

A constant gravitational field has been assumed so that the gravitational force can easily be expressed as

$$\vec{F}_g = \tilde{\rho}gds(\sin\alpha\vec{b}_1 + \cos\alpha\vec{b}_2) \tag{2.12}$$

The expression for the total angle of attack has been reduced to just α since the term $\frac{\partial\zeta}{\partial\varepsilon}$ is very small over most of the hose length.

2.3 TENSILE FORCES

The tensile force in an element of the hose which varies in space and time in the $\vec{b}_2$ direction is given by

$$T_{2x}[\frac{\partial\zeta}{\partial\varepsilon}]_{2x} - T_1[\frac{\partial\zeta}{\partial\varepsilon}]_1 \tag{2.14}$$

The change from 1 to 2 denotes a change in space while the symbol $\times$ denotes a change in time. The tension terms can be written in Taylor series form (with all higher order terms truncated) as

$$T_{2\times} = T_{1\times} + \frac{\partial T}{\partial \varepsilon} d\varepsilon \tag{2.15}$$

$$T_{1\times} = T_1 + \frac{\partial T}{\partial t} dt \tag{2.16}$$

Equation (2.15) represents a step in space while equation (2.16) represents a step in time. Combining equations (2.15) and (2.16) yield

$$T_{2\times} = T_1 + \frac{\partial T}{\partial t} dt + \frac{\partial T}{\partial \varepsilon} d\varepsilon \tag{2.17}$$

The same procedure can be applied to the $\frac{\partial \zeta}{\partial \varepsilon}$ term. After substituting these expressions into equation (2.14) and neglecting the subscripts, the variation in the tensile force becomes

$$[T + \frac{\partial T}{\partial t} dt + \frac{\partial T}{\partial \varepsilon} d\varepsilon][\frac{\partial \zeta}{\partial \varepsilon} + \frac{\partial^2 \zeta}{\partial t \partial \varepsilon} dt + \frac{\partial^2 \zeta}{\partial \varepsilon^2} ds - T\frac{\partial \zeta}{\partial \varepsilon}] \tag{2.18}$$

Expanding equation (2.17) and dropping higher order terms results in

$$T\frac{\partial^2\zeta}{\partial t\partial\varepsilon}dt + T\frac{\partial^2\zeta}{\partial\varepsilon^2}d\varepsilon + \frac{\partial T\partial\zeta}{\partial t\partial\varepsilon}dt + \frac{\partial T\partial\zeta}{\partial\varepsilon\partial\varepsilon}d\varepsilon \tag{2.19}$$

Again it is assumed that the variables ζ and T can each be divided into a pertubation portion and an equilibrium portion. Further simplifying assumptions for the tensile variation are that the tension is time invariant and the perturbation of the tension is small and can therefore be neglected along with its derivatives. If the same approach is followed for the variation of the tension in the ε direction, the total tensile force becomes

$$\vec{F}_T = \frac{\partial\overline{T}}{\partial\varepsilon}d\varepsilon\vec{b}_1 + \tag{2.20}$$

$$[\overline{T}\frac{\partial^2\hat{\zeta}}{\partial\varepsilon^2} + \overline{T}\frac{\partial^2\zeta'}{\partial\varepsilon^2} + \frac{\partial\overline{T}\partial\hat{\zeta}}{\partial\varepsilon\partial\varepsilon} + \frac{\partial\overline{T}\partial\zeta'}{\partial\varepsilon\partial\varepsilon}]d\varepsilon\vec{b}_2$$

The components of the general equation of motion of the hose (2.1) have now been written explicitly. The last contribution to the total dynamic equation is that of elastic bending.

2.4 ELASTIC BENDING

The differential equation of transverse vibration of an Euler-Bernoulli beam is [ref. 4]

$$\frac{\partial^2}{\partial \varepsilon^2}[EI\frac{\partial^2 \zeta}{\partial \varepsilon^2}] + \tilde{\rho}\frac{\partial^2 \zeta}{\partial t^2} = P(\varepsilon, t) \tag{2.21}$$

Here $P(\varepsilon, t)$ represents the net transverse loading acting on the structure and EI is the bending stiffness. Since EI is assumed constant along the hose, equation (2.21) can be written simply as

$$EI\frac{\partial^4 \zeta}{\partial \varepsilon^4} + \tilde{\rho}\frac{\partial^2 \zeta}{\partial t^2} = P(\varepsilon, t) \tag{2.22}$$

Making use of the perturbation and equilibrium portions of the variable ζ gives the expression

$$EI(\frac{\partial^4 \hat{\zeta}}{\partial \varepsilon^4} + \frac{\partial^4 \zeta'}{\partial \varepsilon^4}) + \tilde{\rho}\frac{\partial^2 \zeta'}{\partial t^2} = P(\varepsilon, t) \tag{2.23}$$

Rearranging terms gives

$$\tilde{\rho}\frac{\partial^2\zeta'}{\partial t^2} = P(\varepsilon, t) - EI(\frac{\partial^4\hat{\zeta}}{\partial\varepsilon^4} + \frac{\partial^4\zeta'}{\partial\varepsilon^4}) \tag{2.24}$$

When the components of the aerodynamic, gravitational, and tensile forces are substituted for $P(\varepsilon, t)$ in the above equation, it produces the complete equations of motion of the hose with elastic bending. The resulting differential equation in the ζ direction is

$$- U^2\rho R(C_D + C_F)\sin^2\alpha - U^2\rho RC_F U\sin\alpha \tag{2.25}$$

$$- U^2\rho R[2(C_D + C_F)\sin\alpha\cos\alpha + C_F\cos\alpha](\frac{\partial\hat{\zeta}}{\partial\varepsilon} + \frac{\partial\zeta'}{\partial\varepsilon})$$

$$- U\rho R[2(C_D + C_F)\sin\alpha + 2C_F]\frac{\partial\zeta'}{\partial t} + \tilde{\rho}g\cos\alpha$$

$$+ \bar{T}\frac{\partial^2\hat{\zeta}}{\partial\varepsilon^2} + \bar{T}\frac{\partial^2\zeta'}{\partial\varepsilon^2} + \frac{\partial\bar{T}\partial\hat{\zeta}}{\partial\varepsilon\partial\varepsilon} + \frac{\partial\bar{T}\partial\zeta'}{\partial\varepsilon\partial\varepsilon}$$

$$= \tilde{\rho}\frac{\partial^2\zeta'}{\partial t^2} + EI(\frac{\partial^4\hat{\zeta}}{\partial\varepsilon^4} + \frac{\partial^4\zeta'}{\partial\varepsilon^4})$$

The equilibrium equation in the ε direction is

$$\frac{\partial \bar{T}}{\partial \varepsilon} + \tilde{\rho} g \sin\alpha + U^2 \rho R C_F (\cos^2\alpha - \sin^2\alpha - \sin\alpha)\frac{\partial \hat{\zeta}}{\partial \varepsilon} \tag{2.26}$$

$$+ U^2 \rho R C_F (1 + \sin\alpha)\cos\alpha = 0$$

The equations have now been completely developed for the hose-drogue refueling system for both the elastic bending case and the flexible case.

2.5 EQUILIBRIUM AND PERTURBATION EQUATIONS

The differential equations (2.25) and (2.26) developed in the previous section can be separated into two equilibrium equations, one in each direction, and one perturbation equation in the ζ direction. The equilibrium equation in the ζ direction is given by

$$- U^2 \rho R (C_D + C_F)\sin^2\alpha - U^2 \rho R C_F \sin\alpha \tag{2.27}$$

$$- U^2 \rho R [2(C_D + C_F)\sin\alpha\cos\alpha + C_F \cos\alpha]\frac{\partial \hat{\zeta}}{\partial \varepsilon}$$

$$+ \tilde{\rho} g \cos\alpha + \bar{T}\frac{\partial^2\hat{\zeta}}{\partial\varepsilon^2} + \frac{\partial\bar{T}\partial\hat{\zeta}}{\partial\varepsilon\partial\varepsilon} = EI\frac{\partial^4\hat{\zeta}}{\partial\varepsilon^4}$$

The equilibrium equation in the ε direction is the same as equation (2.26) since there are no perturbation terms present, and it is repeated here for completeness.

$$\frac{\partial\bar{T}}{\partial\varepsilon} + \tilde{\rho} g \sin\alpha + U^2\rho R C_F(\cos^2\alpha - \sin^2\alpha - \sin\alpha)\frac{\partial\hat{\zeta}}{\partial\varepsilon} \tag{2.28}$$

$$+ U^2\rho R C_F(1 + \sin\alpha)\cos\alpha = 0$$

This leaves one perturbation equation (in the ζ direction) which is given by

$$- U^2\rho R[2(C_D + C_F)\sin\alpha\cos\alpha + C_F\cos\alpha]\frac{\partial\zeta'}{\partial\varepsilon} \tag{2.29}$$

$$- U\rho R[2(C_D + C_F)\sin\alpha + 2C_F]\frac{\partial\zeta'}{\partial t}$$

$$+ \bar{T}\frac{\partial^2\zeta'}{\partial\varepsilon^2} + \frac{\partial\bar{T}\partial\zeta'}{\partial\varepsilon\partial\varepsilon} = \tilde{\rho}\frac{\partial^2\zeta'}{\partial t^2} + EI\frac{\partial^4\zeta'}{\partial\varepsilon^4}$$

A mathematical model of the hose dynamics is now completed. The next step is to attempt a solution to these equations and to see how well they represent the physical system.

Chapter 3. Solution of the Equilibrium Equations

In order to solve the perturbation equation and thus observe the hose dynamics, it is necessary to obtain values of some of the parameters in the equations of motion. Throughout this paper all parameters and solutions will be obtained numerically for one test case which is representative of an actual refueling mission between a KC-135 tanker and a U S Air Force fighter aircraft. The constants for this system are listed in Table 1. Most of these come from references 2 and 3, and the value for EI comes from hose stiffness tests in reference 5. The other quantities, such as equilibrium hose angle of attack and equilibrium tension distribution, can be found by solving the equilibrium equations. The equilibrium hose angle of attack at the attachment point is solved for first, and the resulting value is then used to obtain the equilibrium tension distribution solutions for the linear and nonlinear forms of the equations.

3.1 EQUILIBRIUM HOSE ANGLE OF ATTACK

The initial hose angle of attack at the attachment point, α , can be solved for using the equilibrium equation (2.27). At the aircraft attachment point ($\varepsilon = 0$) the hose is very straight and the term $\frac{\partial \hat{\zeta}}{\partial \varepsilon}$ can be set equal to zero (i.e. the slope is zero at the attachment point). The second order derivative $\frac{\partial^2 \hat{\zeta}}{\partial \varepsilon^2}$ is also neglected (i.e. there is no moment at the attachment point as if it were a pin joint). With these simplifications, equation (2.27) becomes

$$-U^2 \rho R(C_D + C_F) \sin^2\alpha - U^2 \rho R C_F \sin\alpha + \tilde{\rho} g \cos\alpha = 0 \qquad (3.1)$$

Equation (3.1) now has only one unknown α which is solved for by finding the roots of the equation and choosing the appropriate value (between 0 and 90 degrees). The equilibrium value for α , using the case values from table one, is 11.4 degrees. This value can now be used in all subsequent equations.

3.2 LINEAR EQUILIBRIUM TENSION DISTRIBUTION

The last step in the equilibrium analysis is the determination of the equilibrium tension distribution. In references 2 and 3 the tension distribution has been *assumed to be* linear so that the tension distribution and its first derivative can

be solved for easily. The same procedure is repeated here, but then the same equations will be solved in their original nonlinear form without assuming a linear distribution. The solutions will then be compared and the assumptions involved will be discussed.

The linear equilibrium tension is found using both equations (2.26) and (2.27) and neglecting all terms higher than first order. This results in the following equations

$$A + \frac{\partial \hat{\zeta}}{\partial \varepsilon}\left(\frac{\partial \overline{T}}{\partial \varepsilon} + B\right) = 0 \tag{3.2}$$

$$\frac{\partial \overline{T}}{\partial \varepsilon} + C + D\frac{\partial \hat{\zeta}}{\partial \varepsilon} = 0 \tag{3.3}$$

A through D are constants for a particular example and are defined as

$$A = -U^2 \rho R[(C_D + C_F)\sin^2\alpha + C_F \sin\alpha] + \tilde{\rho} g \cos\alpha \tag{3.4}$$

$$B = -U^2 \rho R[2(C_D + C_F)\sin\alpha\cos\alpha + C_F \cos\alpha] \tag{3.5}$$

$$C = U^2 \rho R C_F (1 + \sin\alpha)\cos\alpha + \tilde{\rho} g \sin\alpha \tag{3.6}$$

$$D = U^2 \rho R C_F (\cos^2\alpha - \sin^2\alpha - \sin\alpha) \tag{3.7}$$

Equations (3.2) and (3.3) can then be combined to produce a differential equation for the tension given as

$$\frac{d\bar{T}}{d\varepsilon} = \frac{DA - CB}{B + C} \tag{3.8}$$

This equation can be integrated using the boundary condition that the tension at the free end is known. The tension produced at this end is related to the forces acting there created by the drogue and can be expressed as

$$\bar{T}(\varepsilon = l) = W_D \sin\alpha + D_D \cos\alpha \tag{3.9}$$

Integration of equation (3.8) using (3.9) as the boundary condition results in the following expression for linear tension

$$\bar{T} = \frac{\partial \bar{T}}{\partial \varepsilon}(\varepsilon - l) + W_D \sin\alpha + D_D \cos\alpha \tag{3.10}$$

This equation is solved for $\overline{T}$ using the constants from table 1. The tension at the free end of the hose is 453 pounds. Integration yields a tension value of 792 pounds at the attachment point of the hose with a constant slope of approximately 3.5 pounds per foot. A plot of this linear tension distribution is shown in figure 5.

3.3 NONLINEAR EQUILIBRIUM TENSION DISTRIBUTION

The most difficult portion of this research centers around obtaining solutions to the nonlinear form of the equations involving the tension distribution, and this is the point where the research departs from any previous work on this topic. The motivation behind solving these nonlinear equations is to obtain a more accurate solution by making fewer initial assumptions, namely that the higher order terms be retained. Retaining these terms makes the solution much harder to obtain. The method of solution is to put the equations in state space form and then solve the system of equations using appropriate boundary conditions, the selection of which prove to be critical in obtaining converging solutions.

A program called BOUNDSOL was used to solve for two different nonlinear systems of equations, one including the elastic bending terms (called the beam system of equations), and one neglecting any stiffness terms (called the string system of equations) [ref 6]. BOUNDSOL is actually a series of programs

designed to be used as subroutines for a main program written to suit a particular type of problem. It employs a multiple shooting method to solve two point boundary value problems and optimal control problems. The string system of equations, representing the flexible hose model, is solved in addition to the beam system of equations to determine the differences between assuming a flexible hose as opposed to a stiff hose.

3.3.1 String System of Equations

This section is called the "string system of equations" because the differential equations developed for the hose describe a structure which behaves similar to a string. The standard string equation, also known as the wave equation, is a second order partial differential equation which requires two boundary conditions in order to obtain a solution [ref 7]. The boundary conditions for the string equation for the case where one end is fixed and one end is free is that the displacement at the fixed end is zero and the slope at the free end is zero.

The second order differential equations used for the hose model are obtained easily by removing the stiffness term $EI\frac{\partial^4 \zeta}{\partial \varepsilon^4}$ from the equilibrium equations developed in chapter 2. The adjusted form of these equations in each direction are then rewritten in state space form. Three state variables are chosen as

$$X_1 = \overline{T} \tag{3.11}$$

$$X_2 = \hat{\zeta} \tag{3.12}$$

$$X_3 = \frac{\partial \hat{\zeta}}{\partial \varepsilon} \tag{3.13}$$

Here X_1 is the equilibrium tension, X_2 is the transverse displacement of the hose from its equilibrium position, and X_3 is the slope of the displacement curve. Substituting these state variables into the equilibrium equations and rearranging results in a system of three first order differential equations

$$X'_1 = -U^2\rho RC_F(\cos^2\alpha - \sin^2\alpha - \sin\alpha)X_3 \tag{3.14}$$

$$-U^2\rho RC_F(1 + \sin\alpha)\cos\alpha - \tilde{\rho}g\sin\alpha$$

$$X'_2 = X_3 \tag{3.15}$$

$$X'_3 = \frac{1}{X_1}\{U^2\rho R(C_D + C_F)\sin\alpha + U^2\rho RC_F\sin\alpha \tag{3.16}$$

$$- \tilde{\rho} g \cos \alpha + (U^2 \rho R[2(C_D + C_F) \cos \alpha \sin \alpha$$

$$+ C_F \cos \alpha (2 + \sin \alpha)] + \tilde{\rho} g \sin \alpha) X_3$$

$$+ U^2 \rho R C_F (\cos^2 \alpha - \sin^2 \alpha - \sin \alpha) X_3^2 \}$$

This string system of equations requires three boundary conditions rather than two since there are now three first order differential equations instead of one second order differential equation. The two boundary conditions used for a standard string equation can be used here if they are modified for this special case where the string has a mass on the end. In this instance the slope at the end is related to the forces which act on the drogue and cause the slope at the free end to change from zero to a specified equilibrium value. The displacement of the hose at the attachment point is still zero as before, and the third boundary condition is the tension specified at the end to be 453 pounds, as in the linear tension distribution solution. The resulting boundary conditions are summarized here

$$\overline{T}(\varepsilon = l) = W_D \sin \alpha + D_D \cos \alpha \tag{3.17}$$

$$\hat{\zeta}(\varepsilon = 0) = 0 \tag{3.18}$$

$$\frac{\partial \hat{\zeta}}{\partial \varepsilon}(\varepsilon = 1) = \frac{W}{D} - \alpha \tag{3.19}$$

In state space this can be expressed as

$$X_1(\varepsilon = 1) = W_D \sin \alpha + D_D \cos \alpha \tag{3.20}$$

$$X_2(\varepsilon = 0) = 0 \tag{3.21}$$

$$X_3(\varepsilon = 1) = \frac{W}{D} - \alpha \tag{3.22}$$

Solutions to this system of equations were found using BOUNDSOL after much difficulty. The program eventually produced a convergent solution but proved to be very sensitive to the initial guess given. The largest problem encountered was that the program would claim convergence, but the supposed convergent solution would be discontinuous. Apparently the solution would follow a path which was not the correct one and then the solution would have to jump at a node in order to match the boundary

conditions at the end. This problem was reduced by iterating the initial guess values until the jumps decreased in magnitude and were barely visible. The discontinuities could be reduced by this technique but the results were not very reliable since the jumps, although very small, still existed, the convergence rates (such as condition number and absolute error) were poor, and the method of solution at this point was tedious.

Figures 6, 7, and 8 are plots of the three state variables $\overline{T}$, $\hat{\zeta}$, and $\frac{\partial \hat{\zeta}}{\partial \varepsilon}$ versus length of hose. The length of the hose is actually 97 feet but is scaled from 0 to 1 for simplicity. A discontinuity is evident on the plot of the tension distribution at ten percent of the distance along the hose in figure 6.

The next attempt at a solution was to specify the value of tension at the fixed end rather than the free end as one of the boundary conditions. The initial value of the tension at the fixed end was chosen to be the value from the solution obtained when using the previous method of iterating to find the proper initial values. This technique produced converging solutions with no discontinuities and good convergence rates, but was still sensitive to the initial guess. Figures 9, 10, and 11 illustrate the solutions of the state variables versus distance along the hose as before. There are no discontinuities present in any of the plots. Notice that the tension distribution solution to a nonlinear form of the hose equilibrium equations produces a solution which is nearly a straight line. This is similar to the solution obtained from the linear assumption made previously for the same case values except that the initial

value of tension is now 769 pounds rather than 792 pounds and the slope of this line is also slightly different. This means that the actual values of the tension distribution for each case are different, but the behavior of the solutions are very similar.

The fact that the program produces a convergent solution without discontinuities when the equations are integrated forward in space, but the tension is specified at the attachment point, provides the basis for the next approach, which is to integrate backward in space (i.e. from the free end of the hose to the fixed end). This means that the boundary condition of the tension being specified at the end of the hose is now an initial boundary condition rather than a final one. The program prefers this set of boundary conditions since there are now two initial requirements and one final one so that it was easier for the solution to march forward in space and match the one remaining boundary condition at the end of the hose rather than two boundary conditions. The method of integrating backward produces convergence rates which are excellent, and the absolute error rate for this case is on the order of 10^{-8}. The solutions are also less sensitive to the initial guess and do not rely on an initial guess value for the tension at the fixed end of the hose. Plots of the state variables versus distance are shown in figures 12, 13, and 14. They are identical to the three previous figures except that they are mirror images and can be used with sufficient confidence.

3.3.2 Beam System of Equations

The "beam system of equations" is so named because the equations representing the system are similar to those of a vibrating beam. The equations used are the same as those of the string system of equations except the stiffness term with EI is retained. The system is now fourth order and five state variables are chosen in order to put the equations into state space form. These are

$$X_1 = \overline{T} \tag{3.23}$$

$$X_2 = \hat{\zeta} \tag{3.24}$$

$$X_3 = \frac{\partial \hat{\zeta}}{\partial \varepsilon} \tag{3.25}$$

$$X_4 = \frac{\partial^2 \hat{\zeta}}{\partial \varepsilon^2} \tag{3.26}$$

$$X_5 = \frac{\partial^3 \hat{\zeta}}{\partial \varepsilon^3} \tag{3.27}$$

These state variables are substituted into the nonlinear equilibrium equations and produce a system of five first order differential equations which are shown below.

$$X'_1 = -U^2\rho RC_F[(\cos^2\alpha - \sin^2\alpha - \sin\alpha)X_3 \tag{3.28}$$

$$+ (1 + \sin\alpha)\cos\alpha] - \tilde{\rho}g\sin\alpha$$

$$X'_2 = X_3 \tag{3.29}$$

$$X'_3 = X_4 \tag{3.30}$$

$$X'_4 = X_5 \tag{3.31}$$

$$X'_5 = \frac{1}{EI}\{-U^2\rho R\{(C_D + C_F)\sin\alpha + \sin^2\alpha\} \tag{3.32}$$

$$+ \tilde{\rho}g\cos\alpha + \{-U^2\rho R[2(C_D + C_F)\cos\alpha\sin\alpha$$

$$+ C_F \cos\alpha + (1 + \sin\alpha)\cos\alpha] - \tilde{\rho} g \sin\alpha\} X_3$$

$$- U^2 \rho R C_F (\cos^2\alpha - \sin^2\alpha - \sin\alpha) X_3^2 + X_1 X_4\}$$

These five differential equations require five boundary conditions for a solution. The standard boundary conditions used for a pinned-free beam are applied here, again with some modifications to suit the particular problem of having a mass on the end, and the fifth boundary condition used is again to specify the tension at the free end of the hose as 453 pounds. The boundary conditions are summed below

$$\bar{T}(\varepsilon = l) = W_D \sin\alpha + D_D \cos\alpha \tag{3.33}$$

$$\hat{\zeta}(\varepsilon = 0) = 0 \tag{3.34}$$

$$\frac{\partial \hat{\zeta}}{\partial \varepsilon}(\varepsilon = l) = \frac{W \cos\alpha - D \sin\alpha}{W \sin\alpha + D \cos\alpha} \tag{3.35}$$

$$\frac{\partial^2 \hat{\zeta}}{\partial \varepsilon^2}(\varepsilon = 0) = 0 \tag{3.36}$$

$$\frac{\partial^2 \hat{\zeta}}{\partial \varepsilon^2}(\varepsilon = l) = 0 \tag{3.37}$$

In state space this can be expressed as

$$X_1(\varepsilon = l) = W_D \sin \alpha + D_D \cos \alpha \tag{3.38}$$

$$X_2(\varepsilon = 0) = 0 \tag{3.39}$$

$$X_3(\varepsilon = l) = \frac{W \cos \alpha - D \sin \alpha}{W \sin \alpha + D \cos \alpha} \tag{3.40}$$

$$X_4(\varepsilon = 0) = 0 \tag{3.41}$$

$$X_4(\varepsilon = l) = 0 \tag{3.42}$$

Solutions to the tension distribution for this case are obtained in a similar manner as with the string system of equations, and the same difficulties are encountered. First the equations are integrated forward in space and the solutions have discontinuities. Figures 15 through 19 illustrate the five state variables versus distance along the hose for this case. The discontinuities are

small here (after many attempts to iterate the guess values) but are still evident and still create a problem. Next the boundary condition of the tension specified at the free end of the hose is changed to the fixed end and the solutions are continuous but again are extremely sensitive to the initial guess values. Finally the problem is integrated backwards from the free end of the hose to the fixed end and the solutions converge nicely as was the case for the string system of equations. Figures 20 through 24 show the plots for this case. Again they are mirror images of the previous five except that these solutions are much easier to obtain and have excellent convergence criteria. Absolute error is on the order of 10^{-8} and the condition number indicates that the problem is no longer ill conditioned.

The tension distribution for the case of the beam proves to be very similar to the string solution. The value of the tension at the fixed end is 766 pounds as compared to 769 pounds in the string example and 792 pounds for the solution assuming linear tension. The change in slope between the two solutions to the nonlinear equations exists but is negligible.

Chapter 4. Solution of the Perturbation Equation

The equilibrium values of the angle of attack and the tension distribution along the hose have now been solved for three different cases of tension distribution using the example data in Table 1. The perturbation equation may now be solved for this example using these equilibrium values.

4.1 DISCRETIZATION SCHEME

The perturbation equation is a partial differential equation which cannot be solved in closed form so it must be discretized. This is accomplished by using a finite difference approach. The spatial derivatives in the equation are replaced with central difference operators while the time derivatives are left intact. The perturbation equation of motion is repeated here with a change of variable for notation purposes. Let ζ' equal v and rewrite equation (2.29) as

$$- U^2\rho R[2(C_D + C_F)\sin\alpha\cos\alpha + C_F\cos\alpha]\frac{\partial v}{\partial \varepsilon} \tag{4.1}$$

$$- U\rho R[2(C_D + C_F)\sin\alpha + 2C_F]\frac{\partial v}{\partial t}$$

$$+ \bar{T}\frac{\partial^2 v}{\partial \varepsilon^2} + \frac{\partial \bar{T}\partial v}{\partial \varepsilon \partial \varepsilon} = \tilde{\rho}\frac{\partial^2 v}{\partial t^2} + EI\frac{\partial^4 v}{\partial \varepsilon^4}$$

The following finite difference operators are used [ref 8].

$$\frac{\partial v_i}{\partial \varepsilon} = \frac{v_{i+1} - v_{i-1}}{2h} \tag{4.2}$$

$$\frac{\partial^2 v_i}{\partial \varepsilon^2} = \frac{v_{i-1} - 2v_i + v_{i+1}}{h^2} \tag{4.3}$$

$$\frac{\partial^4 v_i}{\partial \varepsilon^4} = \frac{v_{i-2} - 4v_{i-1} - 6v_i - 4v_{i+1} + v_{i+2}}{h^4} \tag{4.4}$$

Substituting equations (4.2) through (4.4) into equation (4.1) yields

$$\ddot{v}_i = \overline{W}\dot{v}_i + \overline{X}(v_{i+1} - v_{i-1}) + \overline{Y}(v_{i-1} - 2v_i + v_{i+1}) \tag{4.5}$$

$$+ \overline{z}(v_{i-2} - 4v_{i-1} - 6v_i - 4v_{i+1} + v_{i+2})$$

The subscript i refers to the position in space. Thus the hose can be divided into n subdivisions where i goes from 0 to n. v_0 is the hose attachment point and v_n is the free end of the hose where the drogue is attached. The terms $\overline{W}$, $\overline{X}$, $\overline{Y}$, and $\overline{Z}$ are listed below.

$$\overline{W} = -\frac{1}{\tilde{\rho}}(\rho RU[2(C_D + C_F)\sin\alpha + 2C_F]) \tag{4.6}$$

$$\overline{X} = \frac{1}{2h\tilde{\rho}}(\frac{\partial \overline{T}}{\partial \varepsilon} \tag{4.7}$$

$$- U^2\rho R[2(C_D + C_F)\sin\alpha\cos\alpha + C_F\cos\alpha])$$

$$\overline{Y} = \frac{\overline{T}}{h^2\tilde{\rho}} \tag{4.8}$$

$$\bar{Z} = -\frac{EI}{h^4\tilde{\rho}} \tag{4.9}$$

The variables $v_i (i = 0 \rightarrow n)$ comprise the state vector {v}. Now the matrix can be written in matrix form with appropriate boundary conditions to eliminate any dependence on the virtual nodes.

The first boundary condition comes from the fact that the perturbation from equilibrium at the aircraft attachment point is zero, so $v_0 = 0$. The virtual node v_{-1} must also be removed from the equation by expressing it in terms of actual nodes. The value at v_{-1} is approximated by assuming that the moment at the attachment point is zero. The moment is expressed as EI times the second derivative with respect to space at v_0 using the central difference operator given below.

$$EI\frac{\partial^2 v_0}{\partial \varepsilon^2} = EI\frac{v_{-1} - 2v_0 + v_1}{h^2} = 0 \tag{4.10}$$

Solving (4.10) for v_{-1} yields

$$v_{-1} = 2v_0 - v_1 \tag{4.11}$$

The boundary conditions at the free end of the hose are found by expressing the slope and bending moment at the end as follows

$$\frac{\partial v_i}{\partial \varepsilon} = \frac{v_{i+1} - v_{i-1}}{2h} = \frac{W}{D} - \alpha \tag{4.12}$$

$$EI\frac{\partial^2 v_i}{\partial \varepsilon^2} = EI\frac{v_{i-1} - 2v_i + v_{i+1}}{h^2} = 0 \tag{4.13}$$

Incorporating these boundary conditions into equation (4.2) removes the expressions of the virtual nodes and results in a matrix form of the perturbation equation which is given below

$$\{\ddot{v}_i\} = \overline{W}\{\dot{v}_i\} + [Q_i]\{v_i\} \tag{4.13}$$

where Q_i is the state matrix consisting of terms which are functions of $\overline{X}$, $\overline{Y}$, and $\overline{Z}$, and these values change for a particular example. This is a second order system and can be reduced to a first order system by introducing a new set of state variables so the dimension of the system doubles. The matrix equation becomes

$$\left\{\frac{\dot{v}}{\ddot{v}}\right\} = \left|\frac{0 \quad I}{Q \quad \overline{W}I}\right| \left\{\frac{v}{\dot{v}}\right\} \tag{4.14}$$

where I is the identity matrix. The perturbation equation has now been written in state space form as $\dot{x} = Ax$ and the hose dynamics can be resolved.

4.2 TIME HISTORIES

The perturbation equation is solved with the different values of the equilibrium tension and hose angle of attack substituted into the discretized model. This model is now in the form of a first order differential equation $\dot{x} = Ax$ in which the states include the displacement of the hose from equilibrium at finite intervals along the length of the hose and the velocities at those same positions. Thus the motion of the hose over time is found by integrating this equation and plotting the results. A Fortran code was written to calculate the hose dynamics and includes a fourth order Runge-Kutta integration scheme.

This procedure is illustrated for two cases, the linear tension case and the beam case, because their boundary conditions are compatible with the system matrix developed in the previous section. The system matrix can be adapted for other sets of boundary conditions easily using the same approach of approximating derivatives with the appropriate finite difference operators. In

each sample case the hose has been divided into five sections giving a total of ten states (five positions and five velocities). The differential equations were both integrated using the set of initial conditions shown in table 2 for this example. The two cases produced almost identical dynamic responses. Plots of the position states versus time are shown in figure 25 and the corresponding velocity states versus time are illustrated in figure 26 for the linear tension distribution case. Similarly, figures 27 and 28 illustrate the dynamic solution for the case of the beam tension distribution.

In each plot the perturbation caused by the initial conditions given takes approximately 20 seconds to damp out completely. The state variable x_5 represents the end of the hose where the drogue is attached. The position of this state over time is the most important to the analysis of this hose-drogue refueling system because its location is critical when performing an inflight refueling mission. The plots show that this state fluctuates the most when compared to the other position states along the hose as expected. In figure 25 the maximum deflection from equilibrium at the free end of the hose is less than 0.4 feet, and figure 27 is identical. The same procedure carried out for different initial conditions produces the same type of dynamic response for the two different tension distributions used in this example. The velocitiy at the end of the hose is also of particular importance. Figures 26 and 28 show the maximum velocity deviation to be just over one foot per second at the free end of the hose (x_{10}). The dynamic response of the hose for this mathematical

model behaves as predicted and damps out after some time due to the aerodynamic damping terms in the equations of motion.

The open loop eigenvalues were calculated for each system matrix and are listed in tables 4 and 5. The values in each case have the same real part. Differences between the two occur in the imaginary part and are in the first decimal position or less so the differences between the eigenvalues of the example system matrices exist but are very small. The system's natural frequencies can be found from the eigenvalues since $\omega = (\sigma^2 + \alpha^2)^{1/2}$ where the ω is the natural frequency and the eigenvalue is expressed as $\sigma + i\alpha$. It is important to know the natural frequencies of the system in order to avoid exciting the system at these frequencies and producing a response which grows over time rather than damping out. In this regard it is important to have as accurate a solution as possible, so it may be advisable to use the more accurate description of the system matrix given by the beam tension distribution for this purpose.

Chapter 5. Conclusions and Recommendations

5.1 CONCLUSIONS

In summary, the hose-drogue refueling system was mathematically modelled using Newton's second law and summing the aerodynamic, gravitational, and tensile forces acting on an element of the hose. The model was then extended to include beam elastic bending effects. The equations of motion developed were then separated into equilibrium and perturbation equations.

The equilibrium equations were used to solve for the equilibrium hose angle of attack and tension distribution. The angle of attack was solved for first, and this value was used when solving for the tension. The nonlinear equations with and without elastic bending were solved in closed form using software. The tension was also assumed to be linear and after discarding terms, this linear approximation was solved also.

Solutions were obtained in each instance using the same case values each time. These values represent a typical refueling mission. The results indicate that the nonlinear equilibrium tension distribution can be solved in closed form after some difficulty, but with excellent convergence criteria. These solutions differ from the solution assuming a linear distribution in the magnitude of the tension along the hose, and thus the slope, but the behavior of all solutions is very similar. The slope (or change in the tension value along the hose) in each case is constant or nearly constant. The value of the tension at the free end of the hose is the same in all cases because it is fixed as a boundary condition.

The most noticeable difference in solutions is the slope of the tension. It is the highest in the linear case and produces the largest value of tension, 792 pounds, at the hose attachment point. The slope of the beam system of equations produces the smallest slope and thus the lowest value of tension, 766 pounds, at the fixed end. The string system of equations has a slope very close to the beam system of equations with a tension of 769 pounds. This data is tabulated in table three. The maximum difference in tension magnitude occurs at the hose attachment point. Here there is a difference in values between the linear solution and the nonlinear beam solution of less than 4 percent. There is of course a 0 percent difference at the free end so the difference in solutions of the magnitude of the tension whould never exceed 4

percent in this case, and will be less when considering the change in magnitude at other points along the hose.

These results show that the tension distribution can be solved more accurately by finding a closed form solution to the nonlinear equations, but this solution is sufficiently close, in magnitude and in behavior, to the solution of the linearized equations. It is recommended that the linear approximation be used for most instances because of the simplicity in obtaining its solution. This solution can also be used with confidence because it has been shown that the assumptions involved are valid and still produce reliable results.

The solutions to the perturbation equation were obtained using the linear equilibrium tension distribution and the tension distribution corresponding to the beam system of equations. Both cases produce almost identical dynamic responses and further validate the recommendation that the linear equilibrium tension distribution solution be used in the analysis of this refueling system; however, the solution to the nonlinear equilibrium equations may be useful when solving for the open loop eigenvalues of the system because even slight differences become important when calculating natural frequencies.

5.2 RECOMMENDATIONS

One purpose of this research was to develop an accurate structural model of the hose-drogue refueling system. The model used herein produced reliable results but could be improved upon in several ways.

A more accurate model could be to include the drogue dynamics in the equations of motion. The equations developed previously only included the effects of the drogue in the boundary conditions. This approach is not entirely valid because the drogue has significant mass and aerodynamic forces acting on it which influence the behavior of the hose all along its length rather than just in the vicinity of the drogue attachment point. The problem associated with solving this system of equations is that it becomes sufficiently complex enough to create difficulties when attempting a solution to the nonlinear equilibrium equations in closed form. The problem may well be ill conditioned and a convergent solution unlikely.

The structural model could also be further analyzed by using a finite element approximation to discretize the system rather than a finite difference scheme. The results from the two methods of solution and the numerical errors involved could be compared.

Another addition to this research would be to implement a control system for the hose so that any oscillations could be quickly damped out. One way to accomplish this task would be to place a control device, such as flaps, at the free end of the hose where the drogue is attached. This would enable the drogue to remain in a steady position relative to the aircraft, even in the presence of atmospheric disturbances.

A last recommendation would be to realize that the true structure involved is, in reality, very different from a string or a beam. The actual physical system is not infinitely flexible because it does have some measure of stiffness, but it does not behave as a beam, either. Its cross section is unusual; circular and hollow in the center. In reality the true system lies somewhere between the string and beam approximations, but most importantly, its solution may not.

List of References

1. Air Force Technical Report AR 83-003,"KC-135 Fuselage Hose Reel System", April 15, 1983.

2. DeLaurier, J. D. and Lowe, J. D., "Stability Analysis of the KC-135A Hose-Drogue Aerial Refueling System: Phase I", December, 1982.

3. DeLaurier, J. D. and Lowe, J. D., "Stability Analysis of the KC-135A Hose-Drogue Aerial Refueling System: Phase II", February, 1983.

4. Craig, R. R. Jr., "Structural Dynamics: An Introduction to Computer Methods", 1981 by John Wiley and Sons, Inc., pp. 192-198.

5. Monfort, J. B., et. al.,Air Force Technical Report AFWAL-TR-85- 3058, "KC-135A Aerial Refueling Hose Longitudinal Stiffness Tests", December, 1985.

6. Cliff, E. M., and Bilimoria, k., " A Primer on OPTSOL ", July 1983, VPI and SU research supported under grant NAG-1-203 from NASA Langley Research Center.

7. Boyce, W. E., and DiPrima, R. C., "Elementary Differential Equations and Boundary Value Problems", 1977 by John Wiley and Sons, pp. 491-499.

8. Gerald, C. F., and Wheatley, P. O., "Applied Numerical Analysis", 1985 by Addison-Wesley, pp. 243-244.

Tables

Table 1: Hose-Drogue Refueling System Data

Length L	97 ft
Radius R	0.1615 ft
Altitude	10,000 ft
Tow Speed U	506 ft / sec
Hose Density	3.5 lb / ft
C_D	1.2
W_D	63 lb
C_{DD}	2.0
D_D	449.5 lb
C_F	0.0283
EI	4600 lb ft^2

Table 2: Initial Conditions

x_1	0.0
x_2	0.5
x_3	1.0
x_4	0.5
x_5	0.0
x_6	0.0
x_7	0.5
x_8	1.0
x_9	0.5
x_{10}	0.0

Table 3: Equilibrium Tension Distribution Results

	$T(\varepsilon = 0)$	Slope
Linear	792	3.495
String	769	3.258 (ave)
Beam	766	3.227 (ave)

Table 4: Open Loop Eigenvalues; Linear Model

-0.3145	6.7142 i
-0.3145	-6.7142 i
-0.3145	5.5667 i
-0.3145	-5.5667 i
-0.3145	4.3110 i
-0.3145	-4.3110 i
-0.3145	3.1532 i
-0.3145	-3.1532 i
-0.3145	2.5861 i
-0.3145	-2.5861 i

Table 5: Open Loop Eigenvalues; Beam Model

-0.3145	6.6110 i
-0.3145	-6.6110 i
-0.3145	5.5039 i
-0.3145	-5.5039 i
-0.3145	4.2690 i
-0.3145	-4.2690 i
-0.3145	3.1213 i
-0.3145	-3.1213 i
-0.3145	2.5526 i
-0.3145	-2.5526 i

Figures

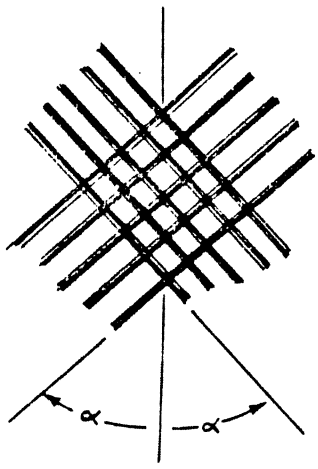

Hose Criss-Cross Pattern of Wire Braid

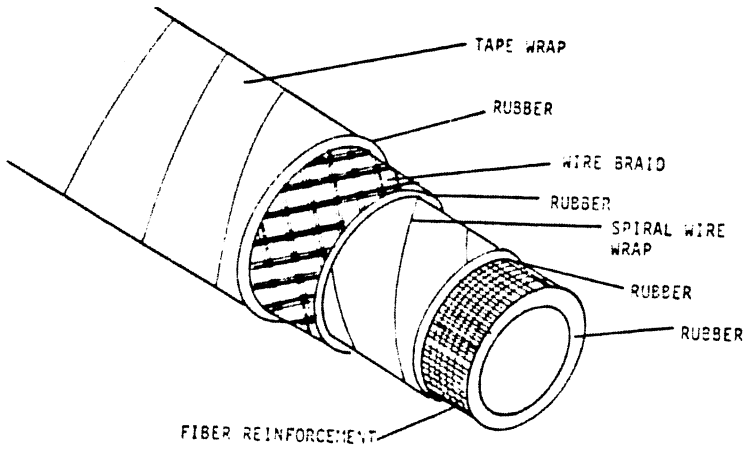

Construction of Hose

Figure 1 Refueling Hose Configuration

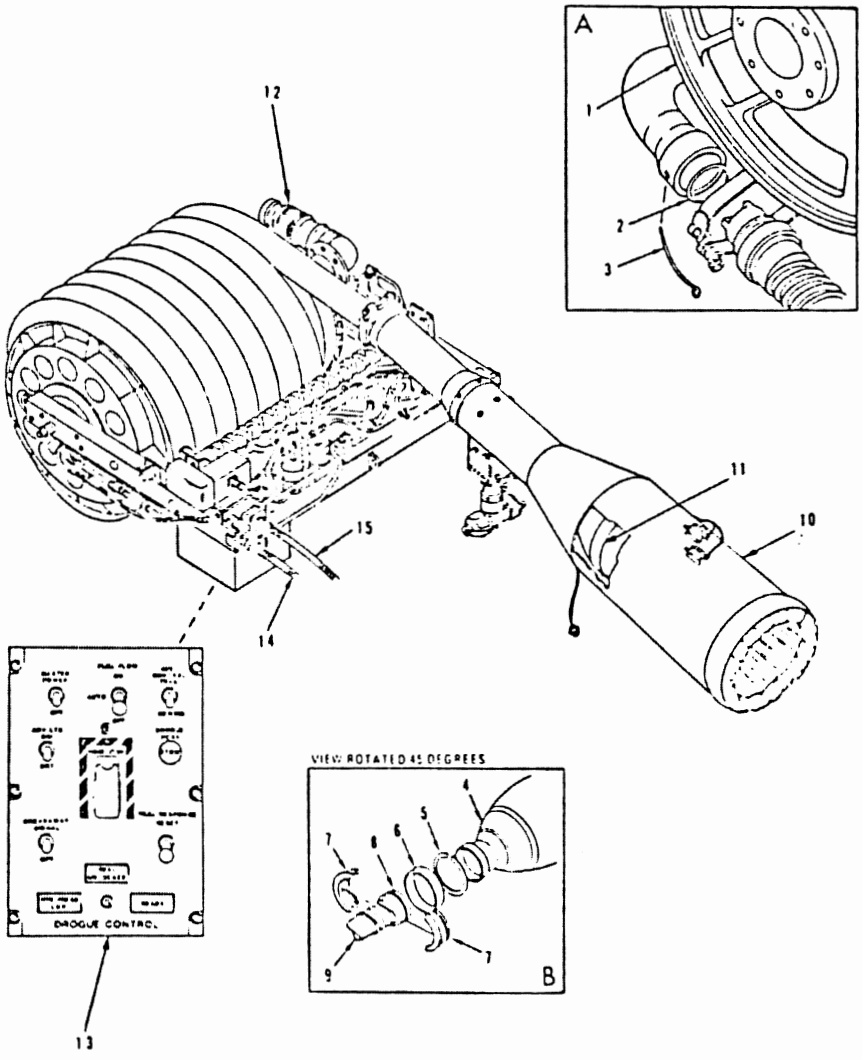

Figure 2 Hose-Drogue Reel Assembly

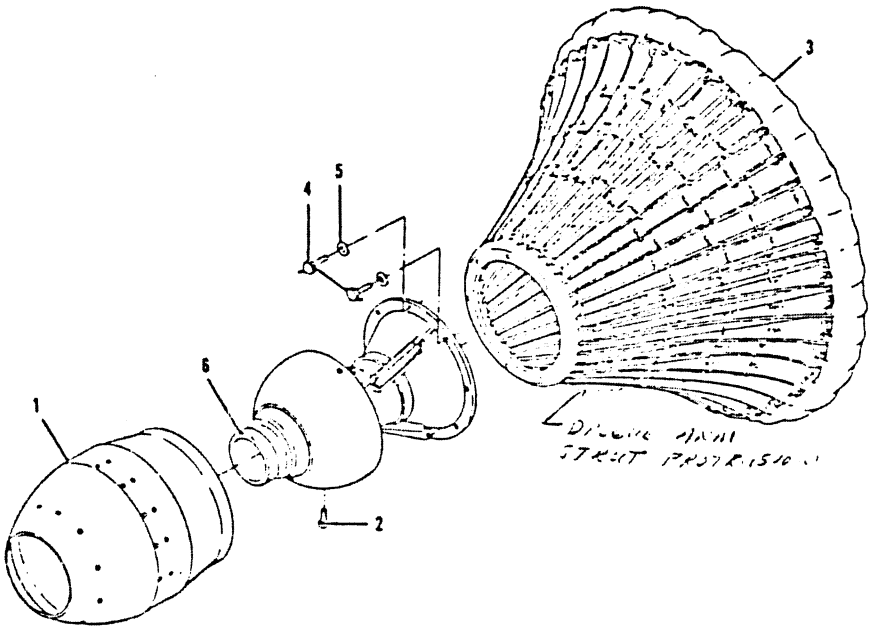

Figure 3 Drogue Configuration

Local Coordinate System

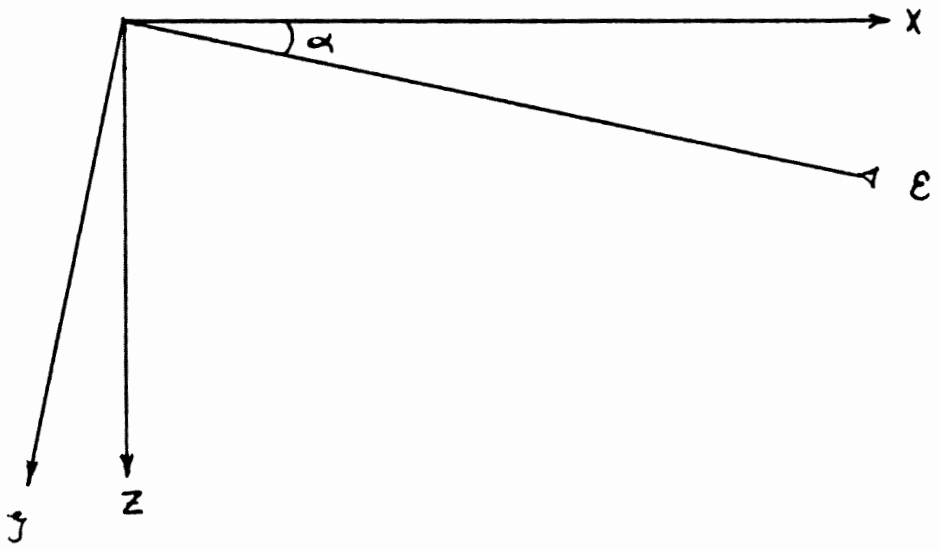

Figure 4 Local Coordinate System

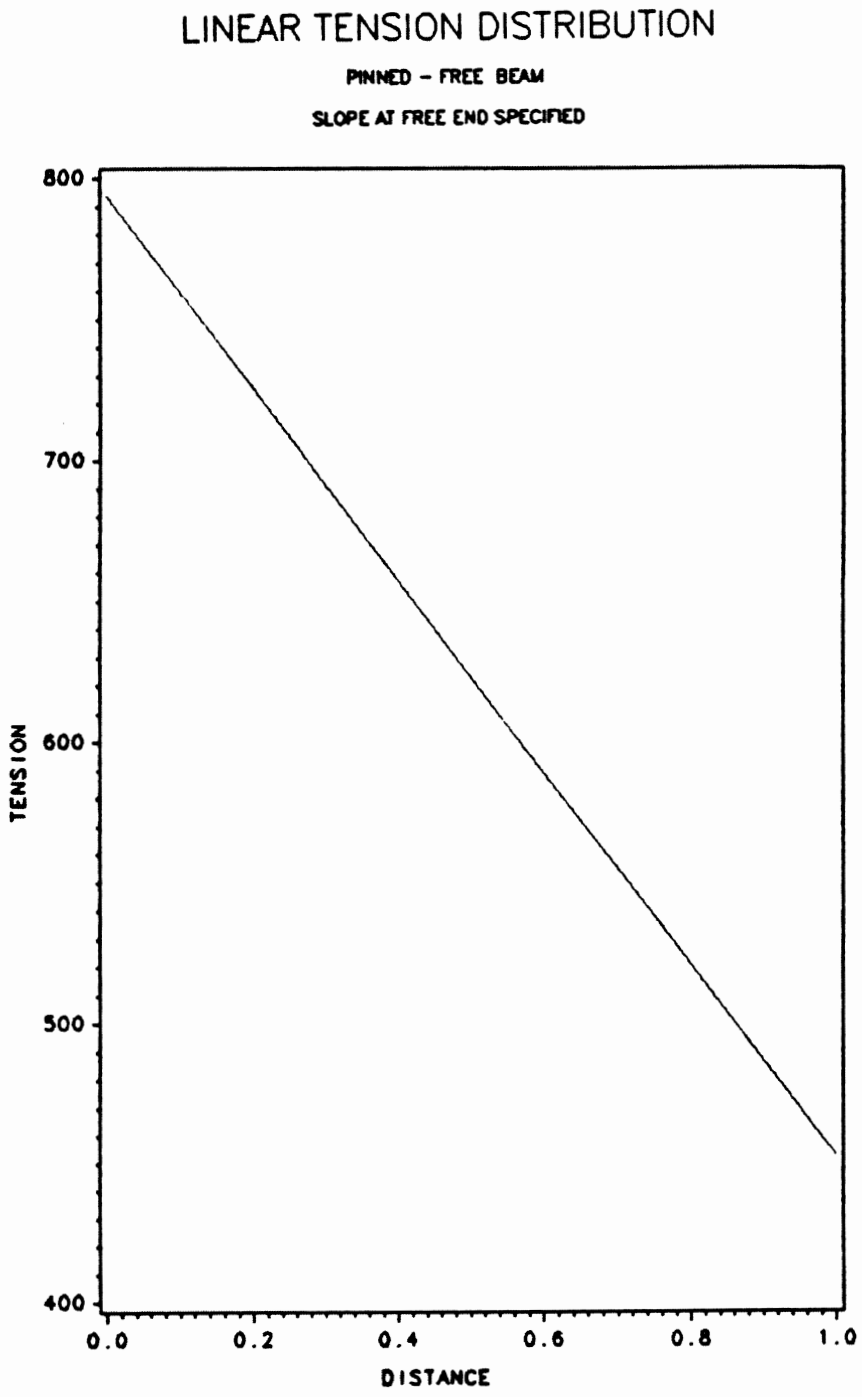

Figure 5 Tension Distribution; Linear Model

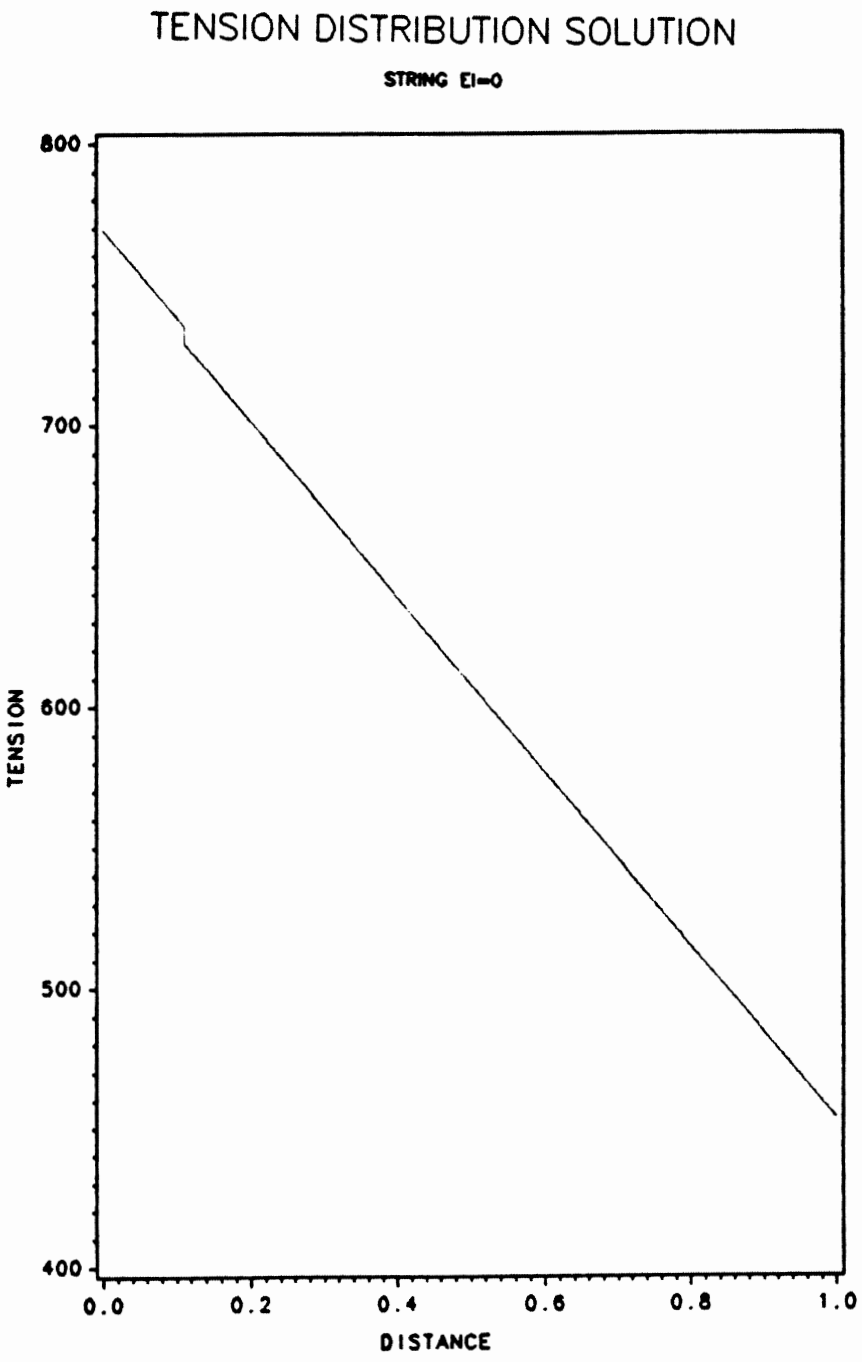

Figure 6 Tension Distribution; String Model (dis)

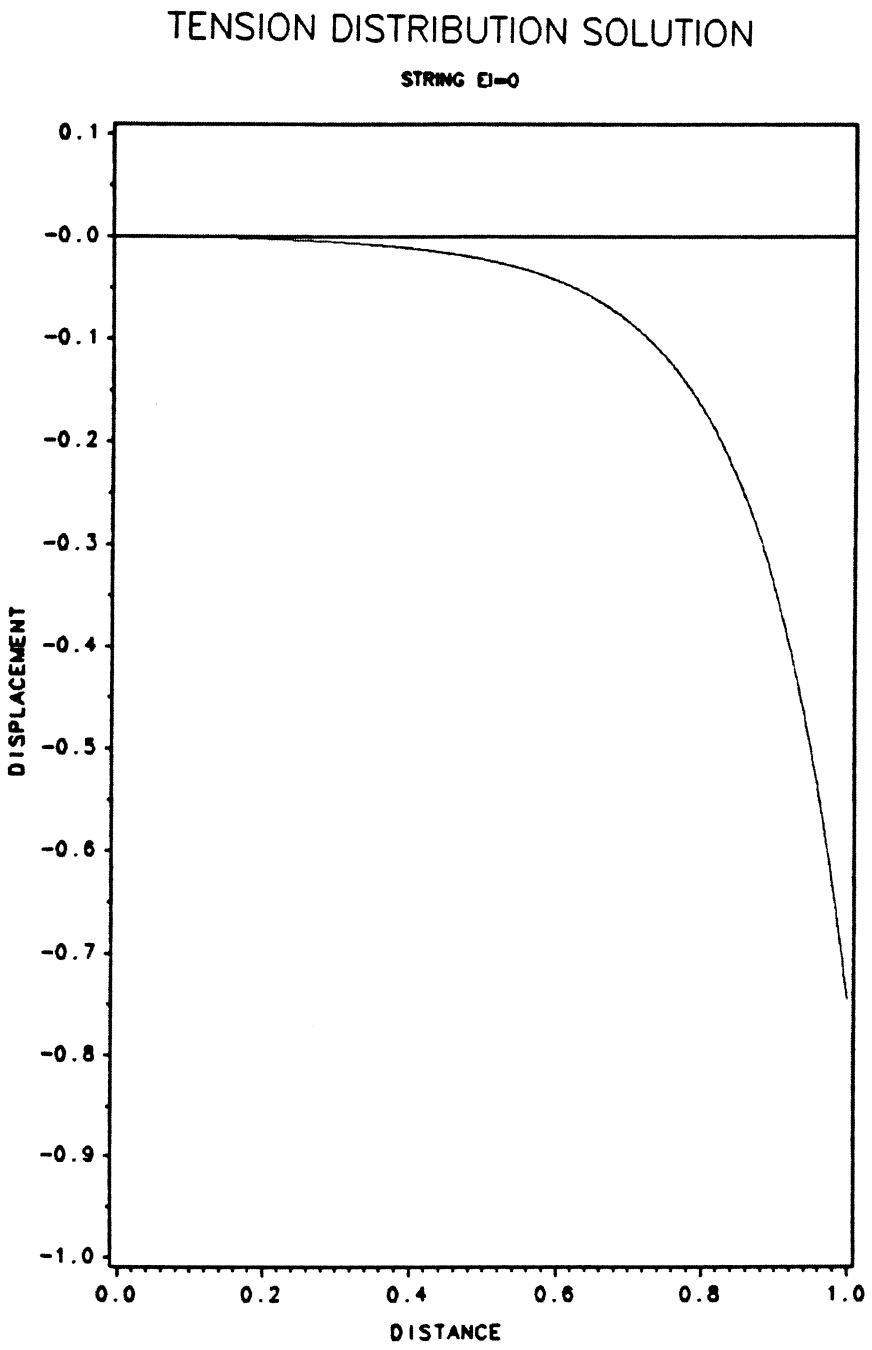

Figure 7 Displacement ζ; String Model (dis)

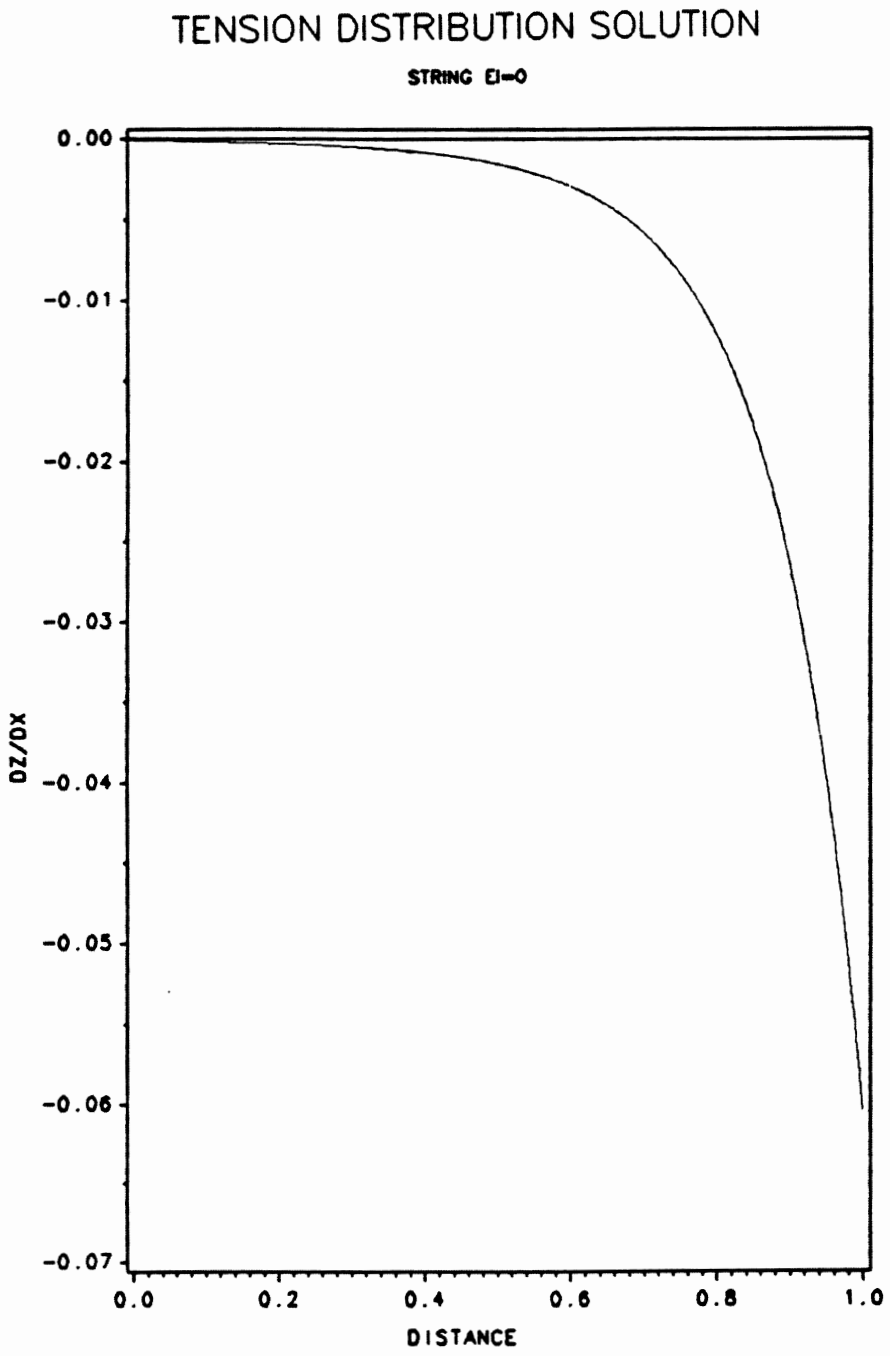

Figure 8 Slope $\frac{\partial \zeta}{\partial \varepsilon}$; String Model (dis)

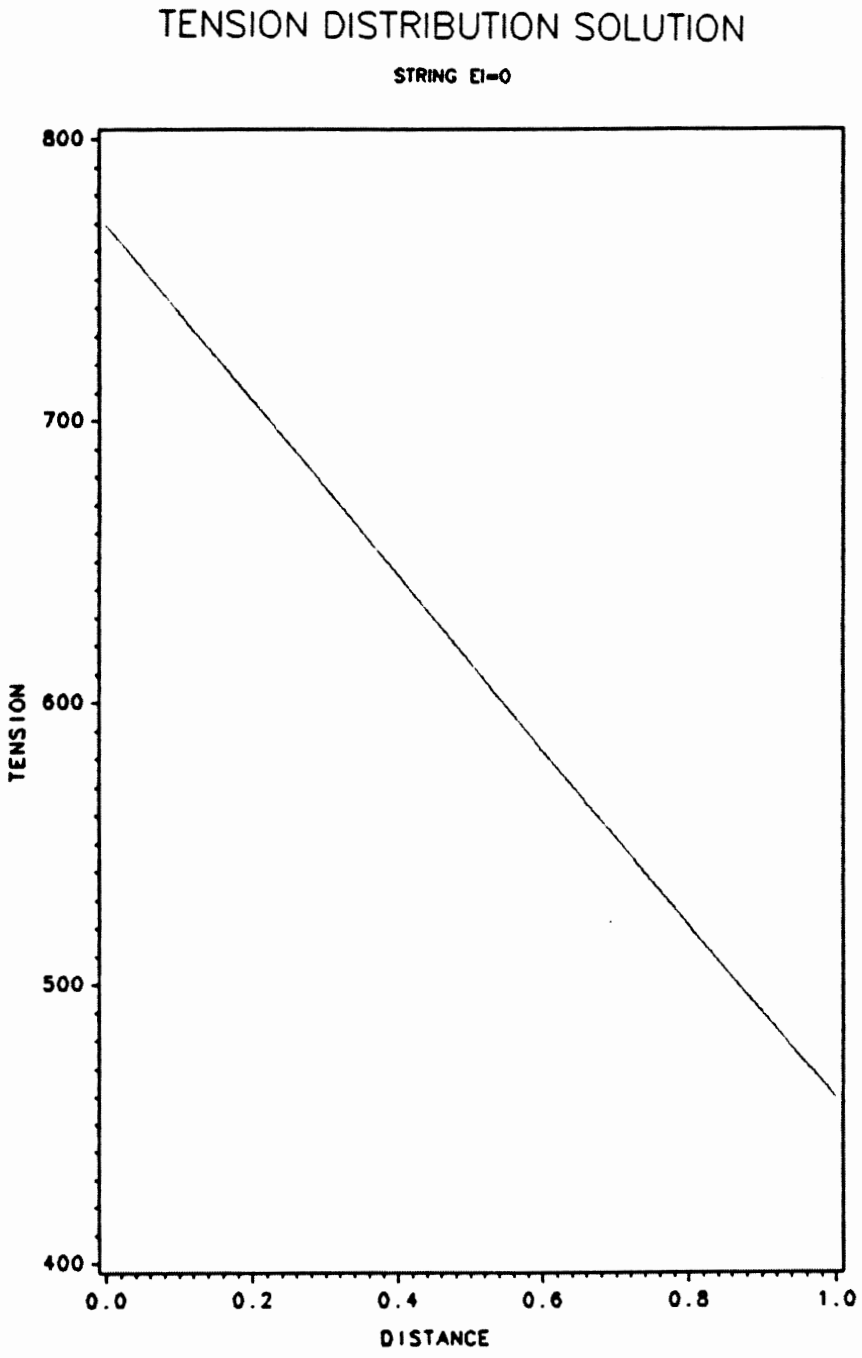

Figure 9 Tension Distribution; String Model

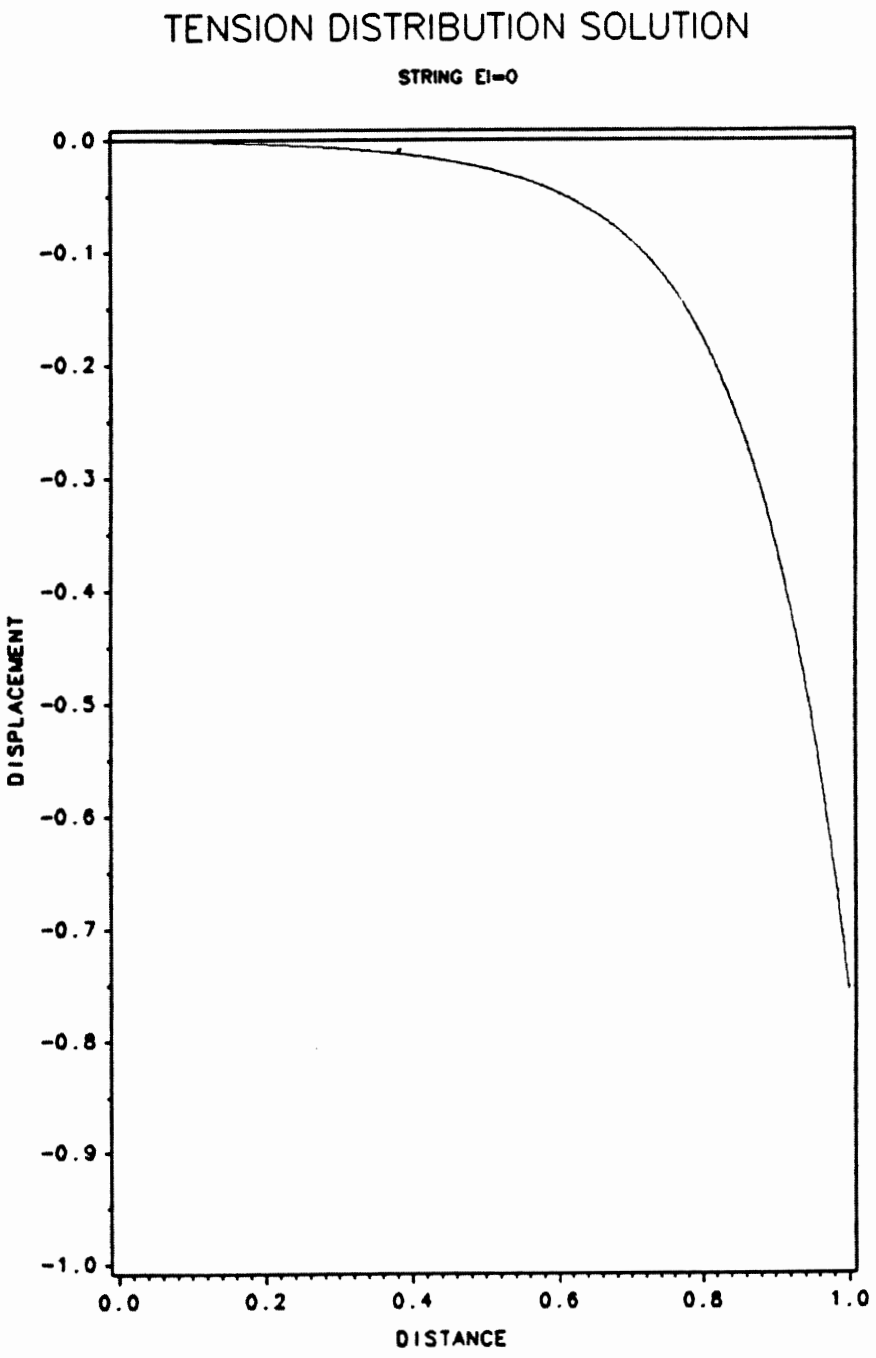

Figure 10 Displacement ζ; String Model

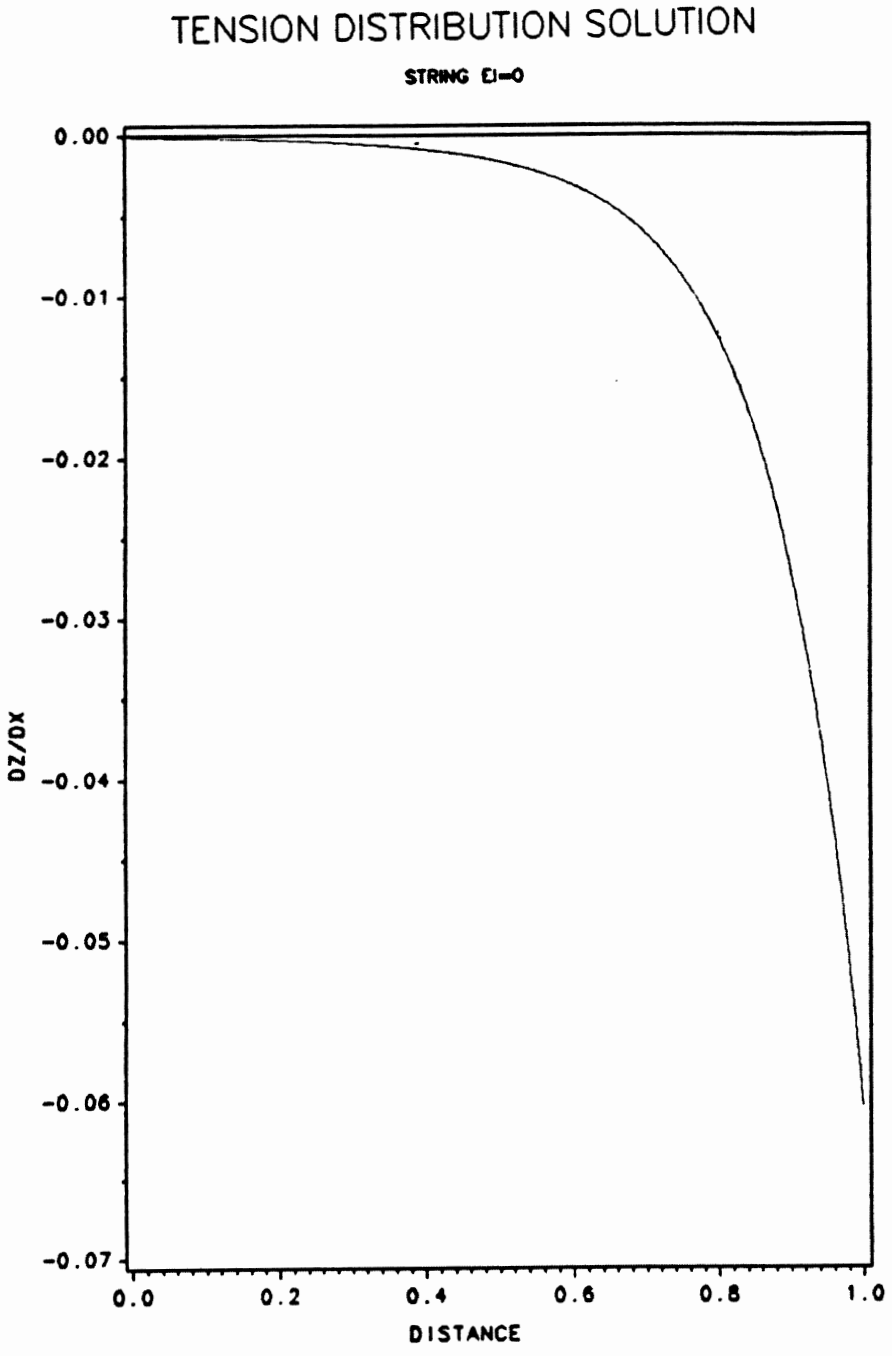

Figure 11 Slope $\frac{\partial \zeta}{\partial \varepsilon}$; String Model

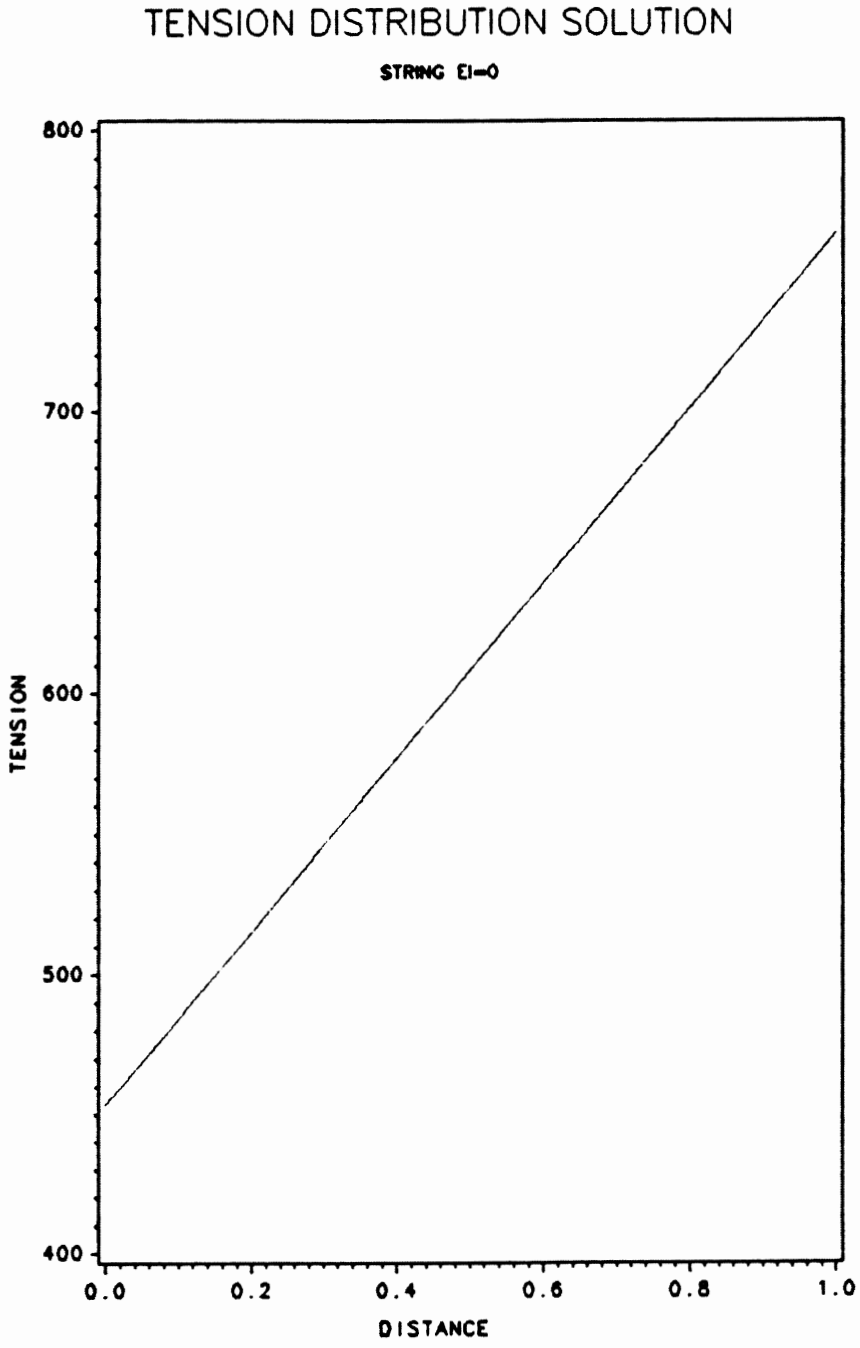

Figure 12 Tension Distribution; String Model (back)

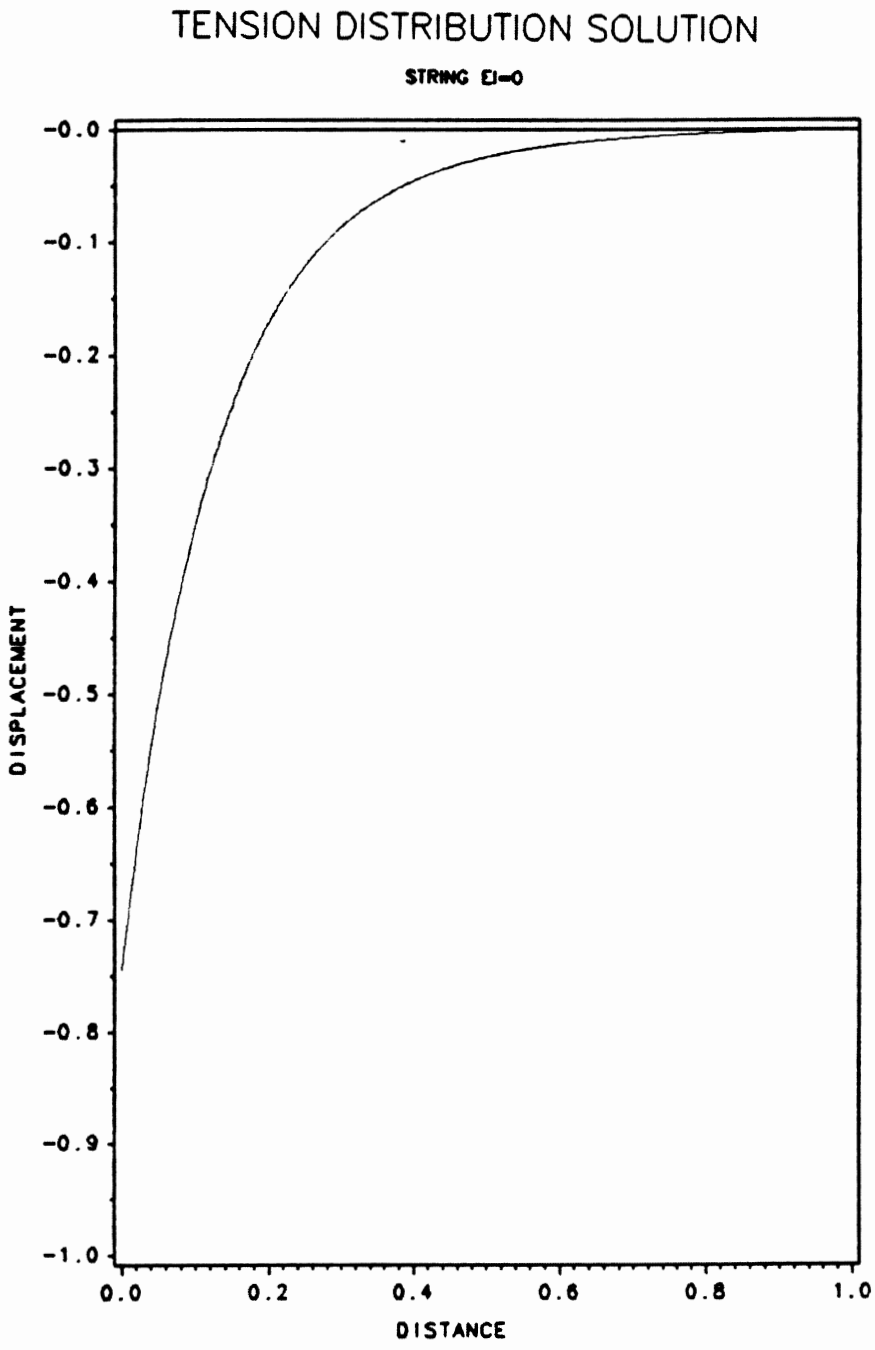

Figure 13 Displacement ζ; String Model (back)

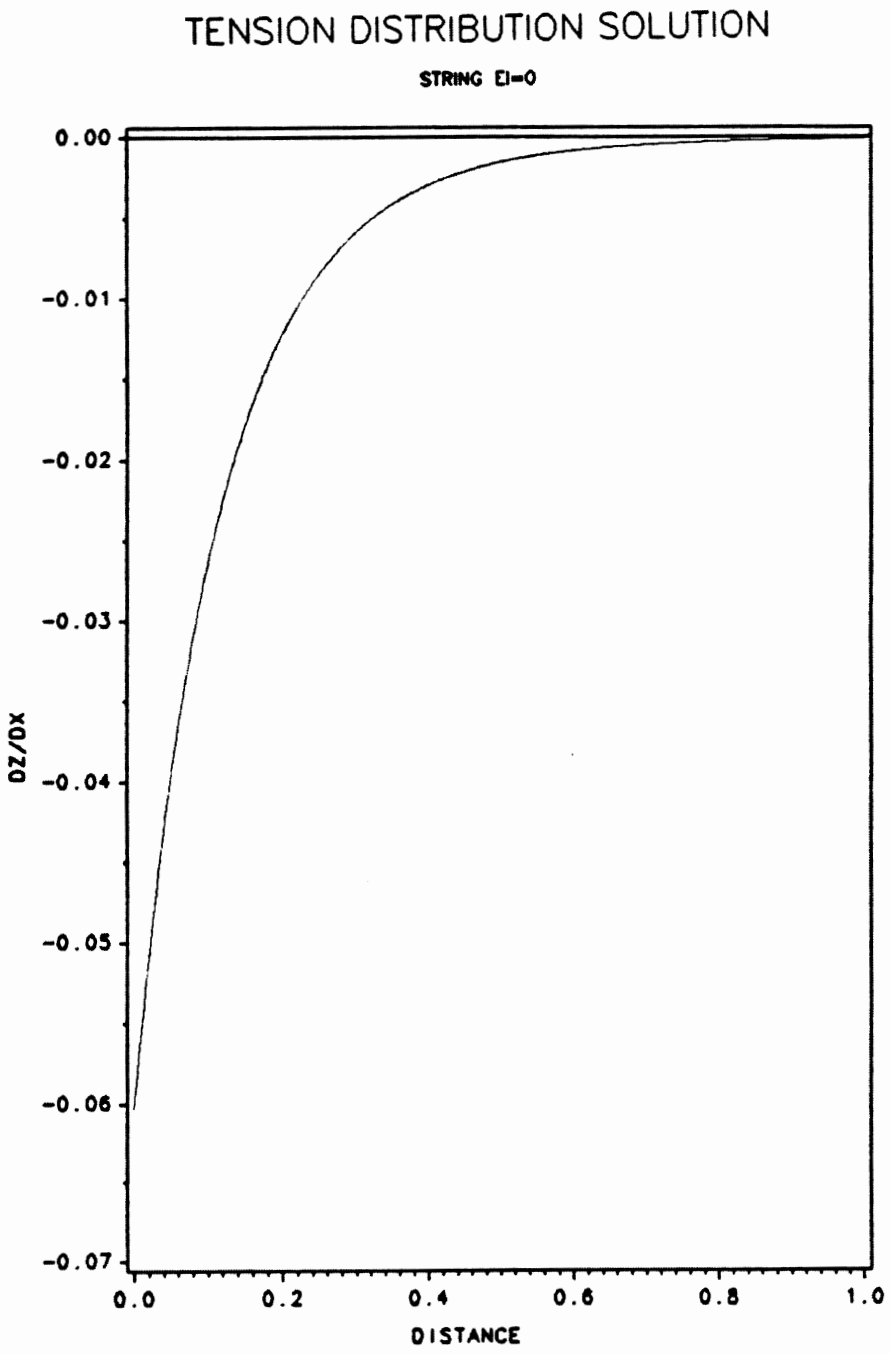

Figure 14 Slope $\frac{\partial \zeta}{\partial \varepsilon}$; String Model (back)

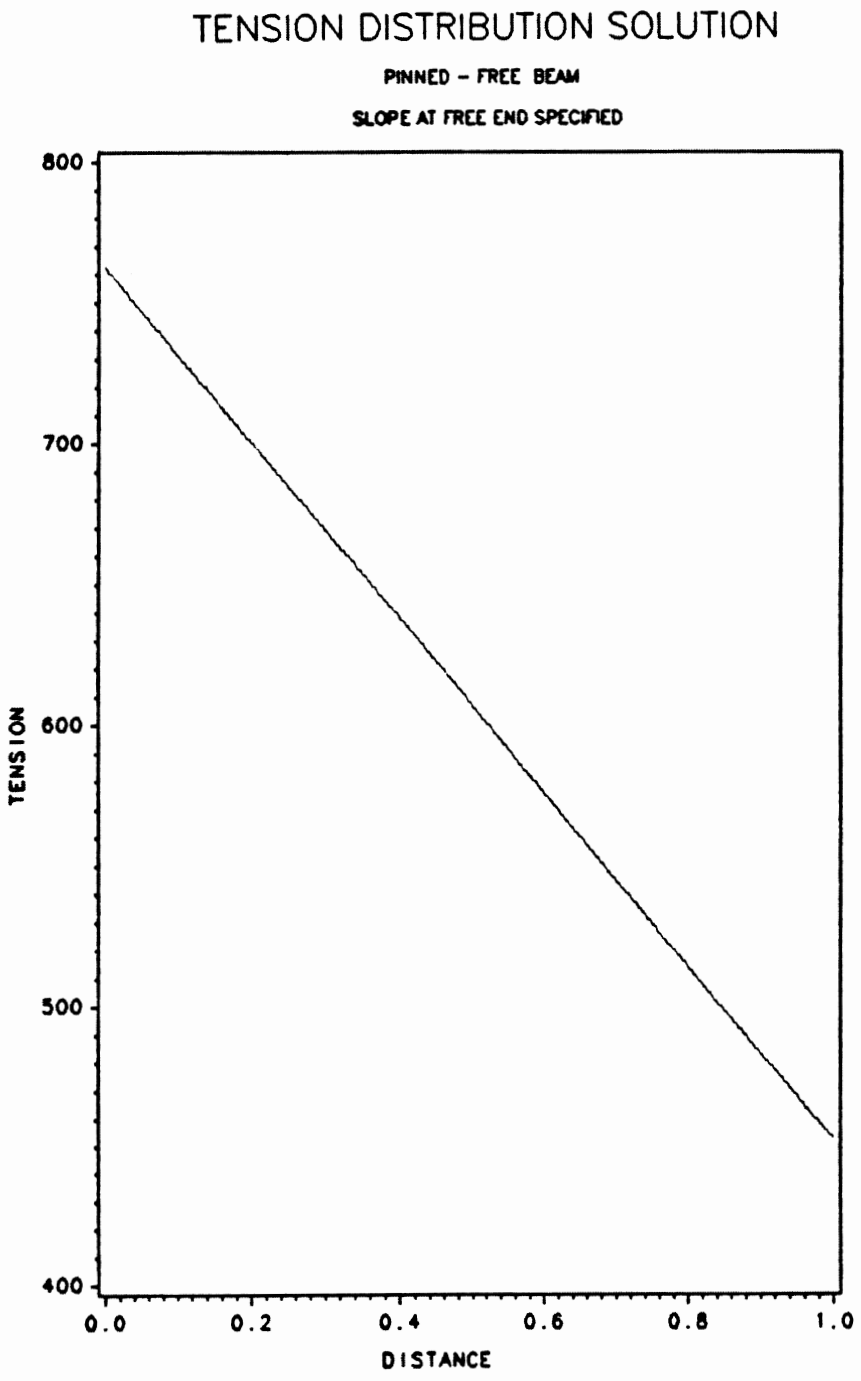

Figure 15 Tension Distribution; Beam Model (dis)

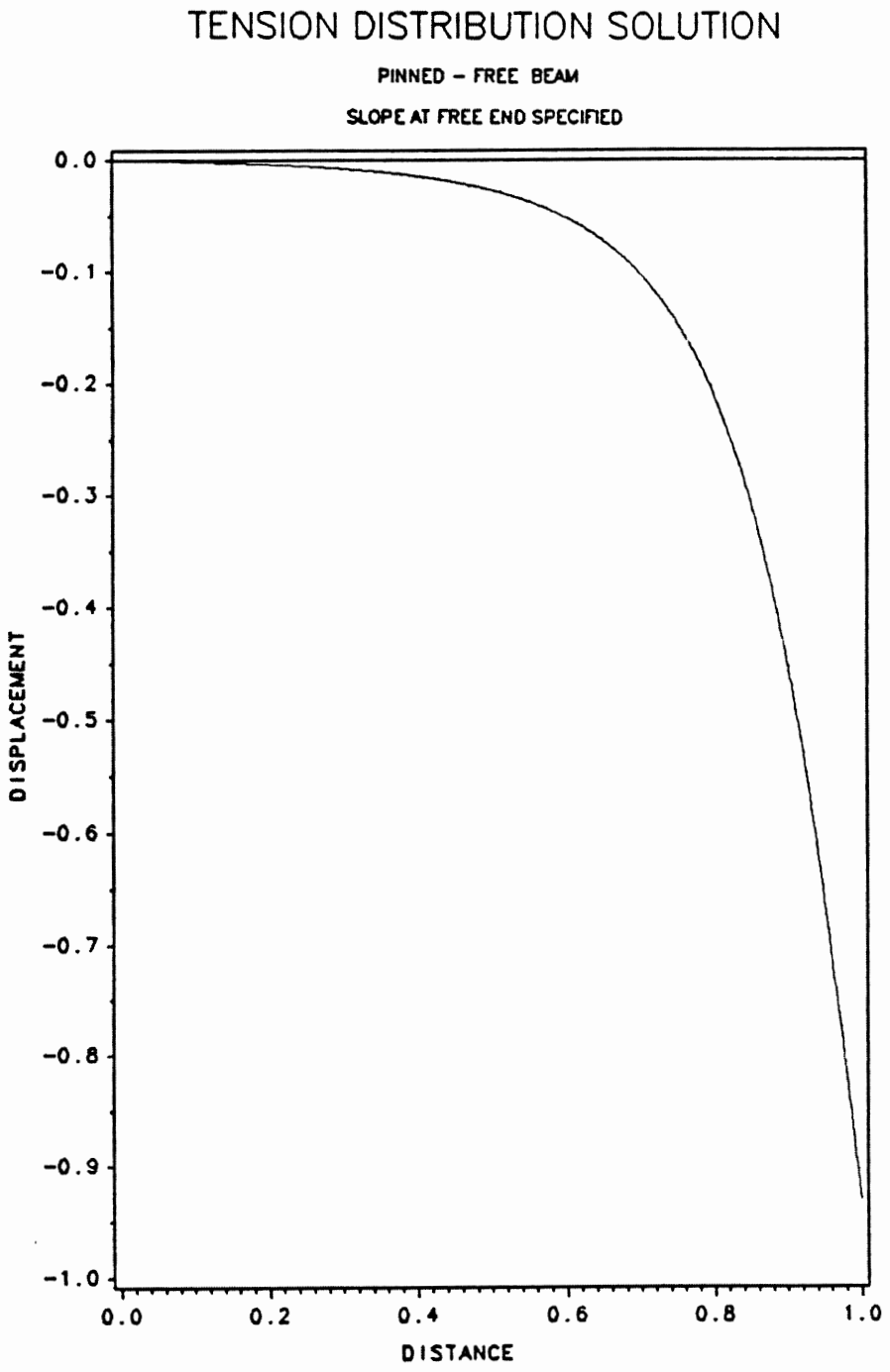

Figure 16 Displacement ζ; Beam Model (dis)

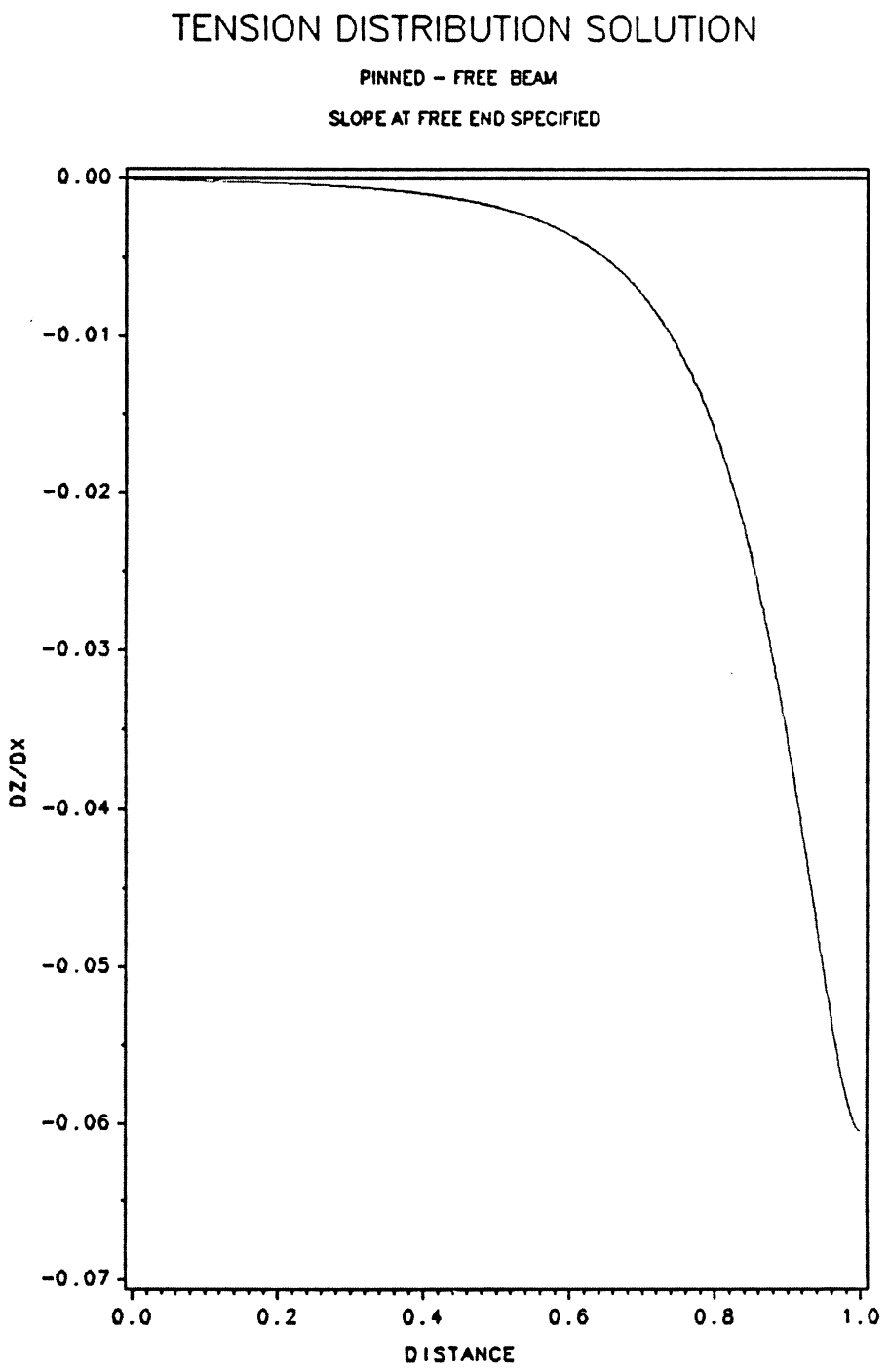

Figure 17 Slope $\frac{\partial \zeta}{\partial \varepsilon}$; Beam Model (dis)

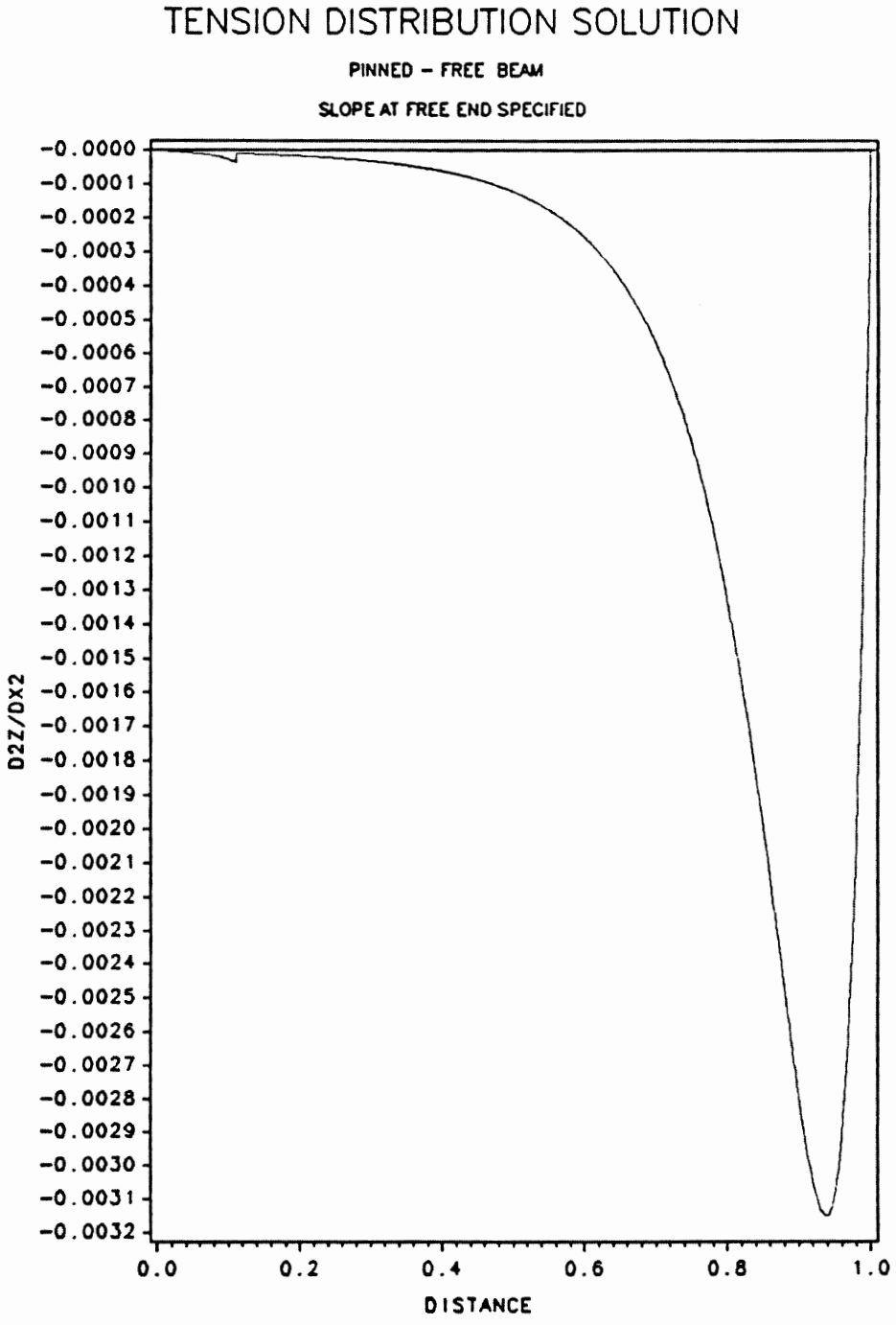

Figure 18 $\frac{\partial^2 \zeta}{\partial \varepsilon^2}$; Beam Model (dis)

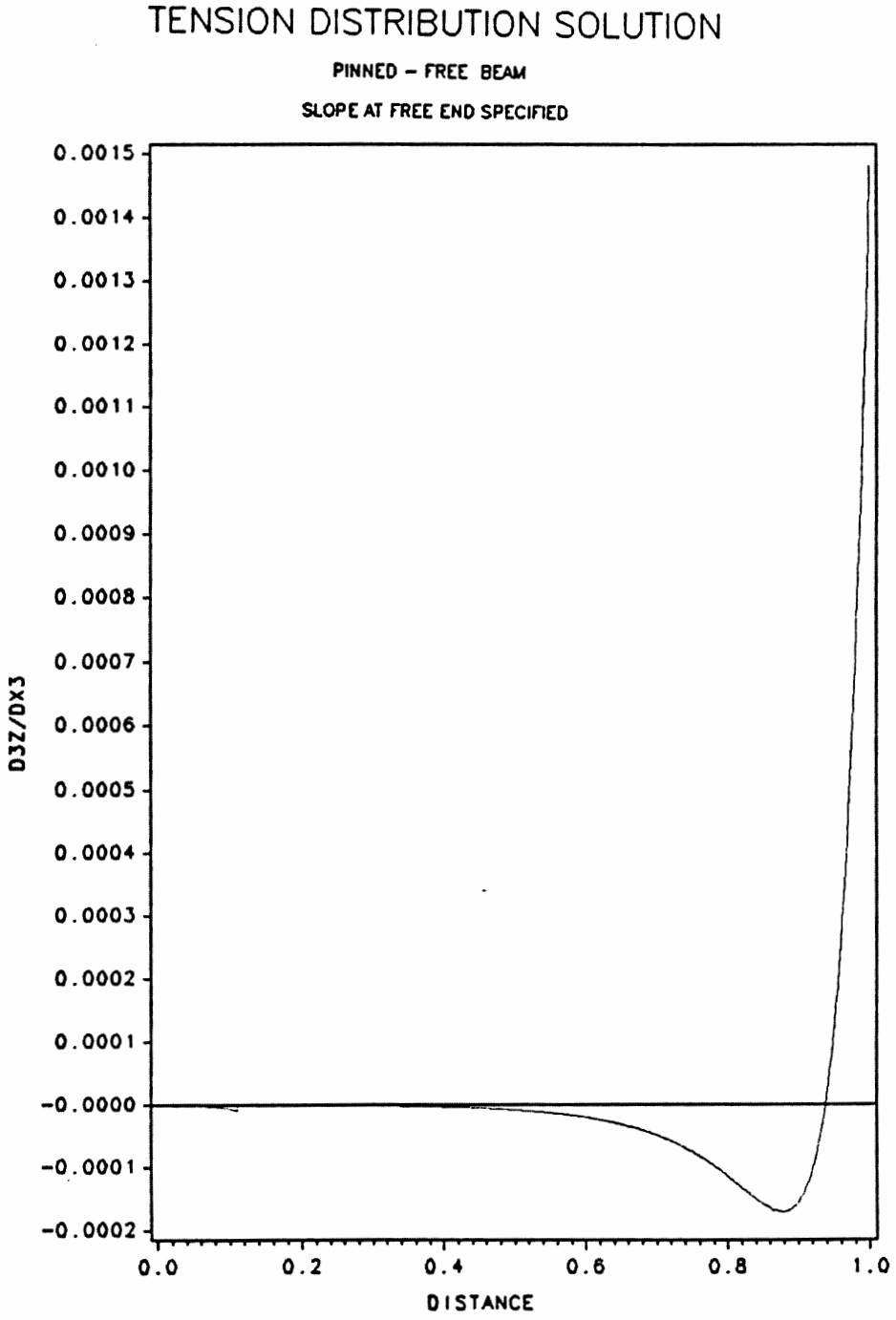

Figure 19 $\frac{\partial^3 \zeta}{\partial \varepsilon^3}$; Beam Model (dis)

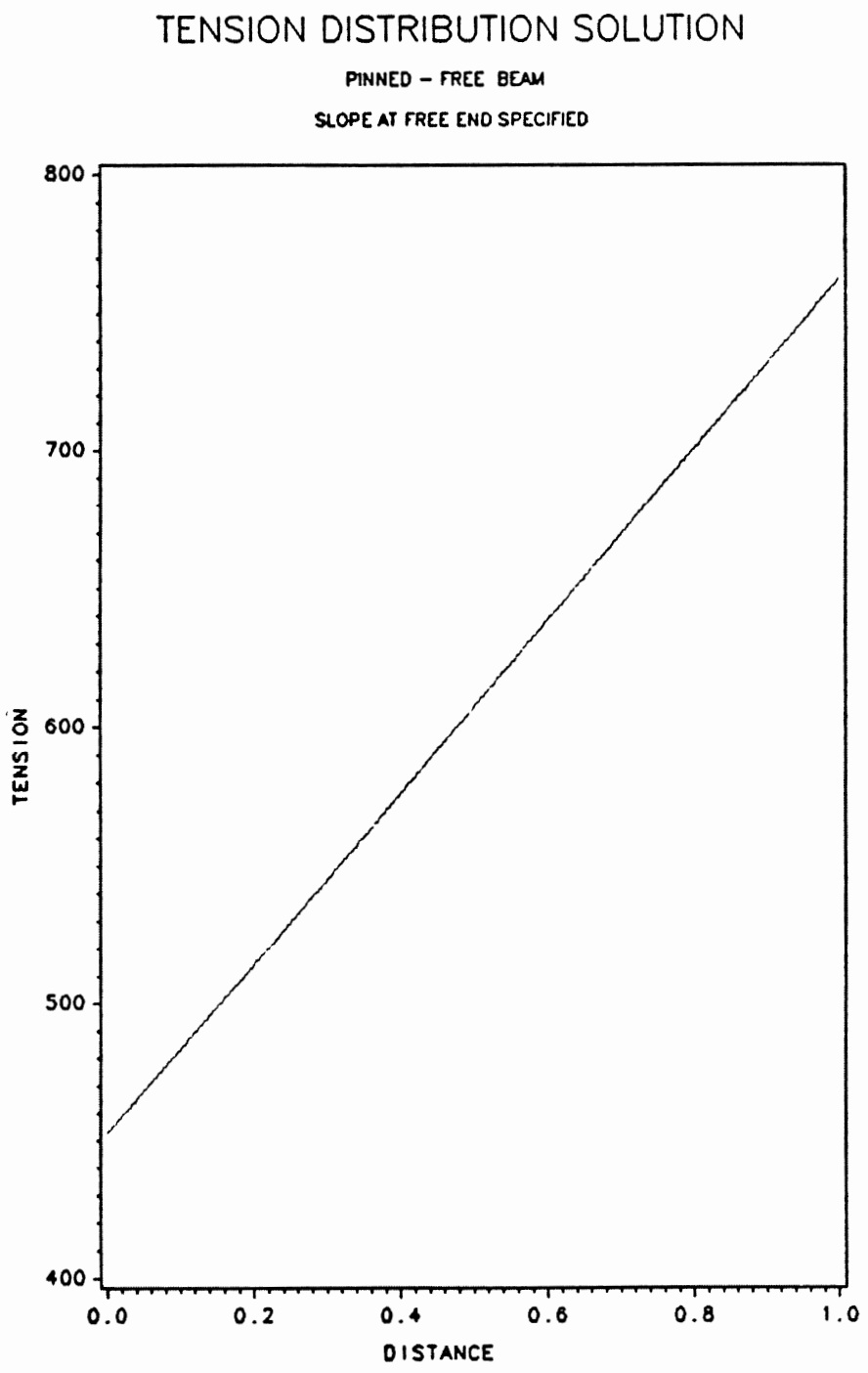

Figure 20 Tension Distribution; Beam Model (back)

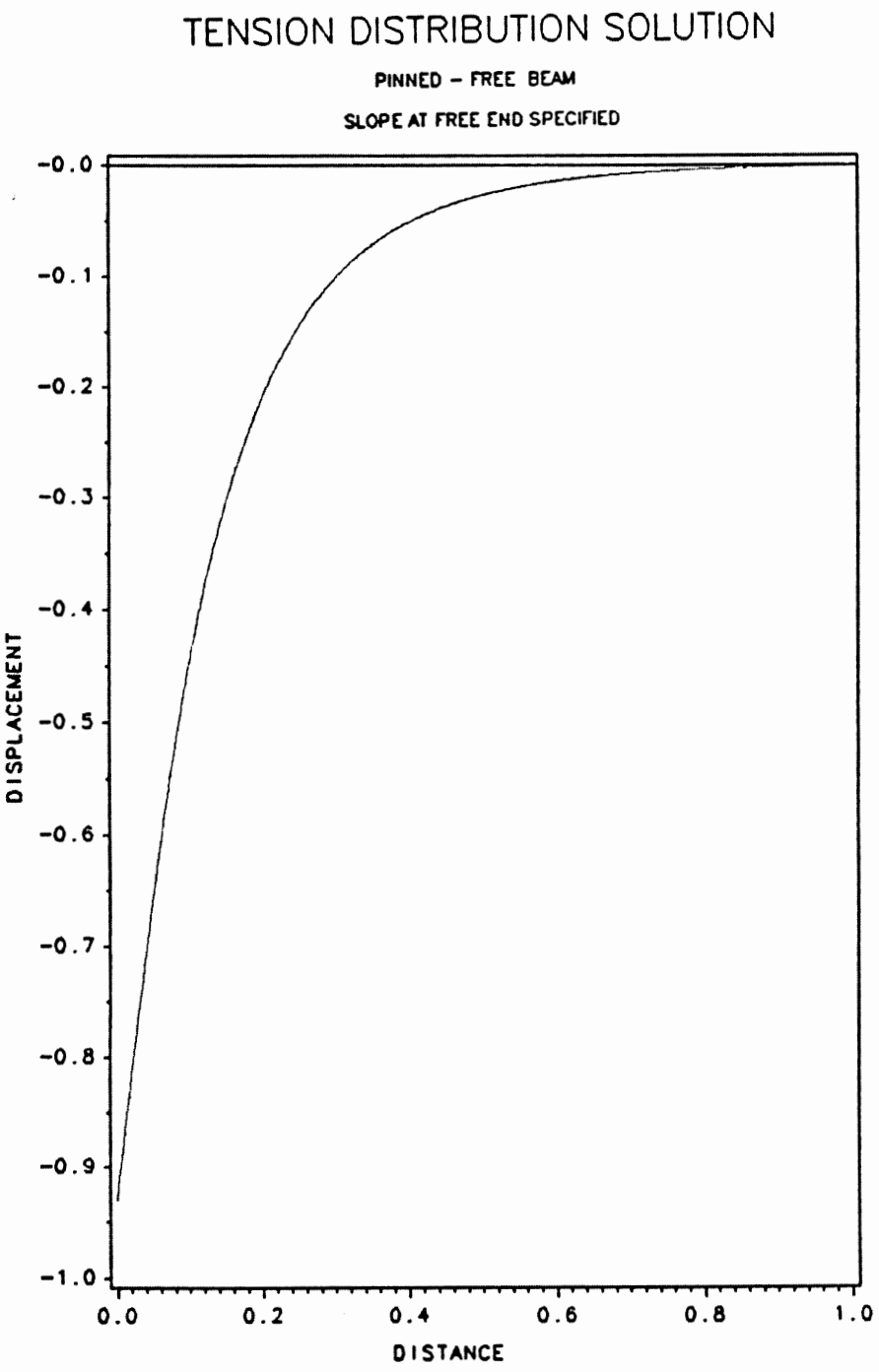

Figure 21 Displacement ζ; Beam Model (back)

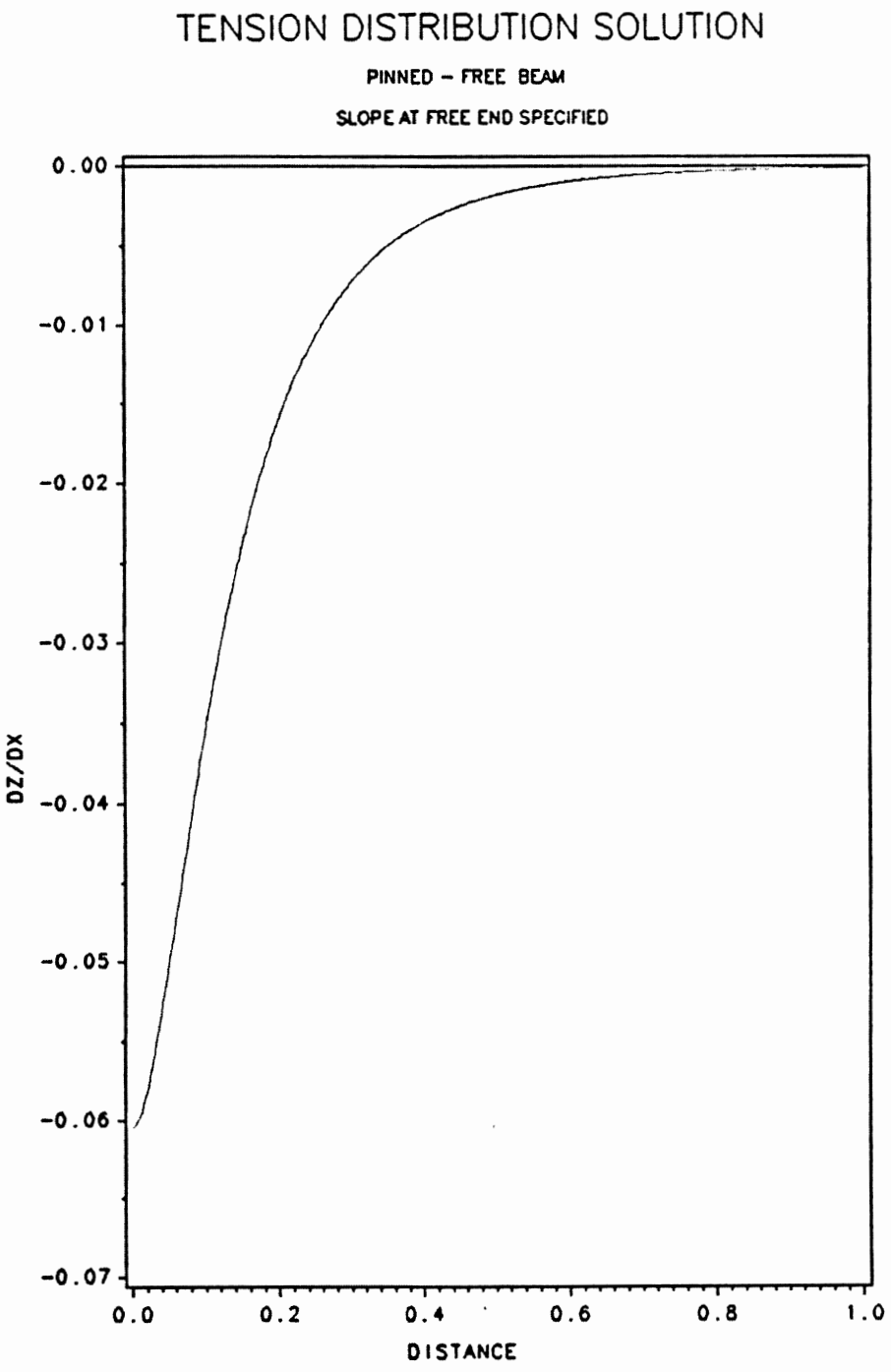

Figure 22 Slope $\frac{\partial \zeta}{\partial \varepsilon}$; Beam Model (back)

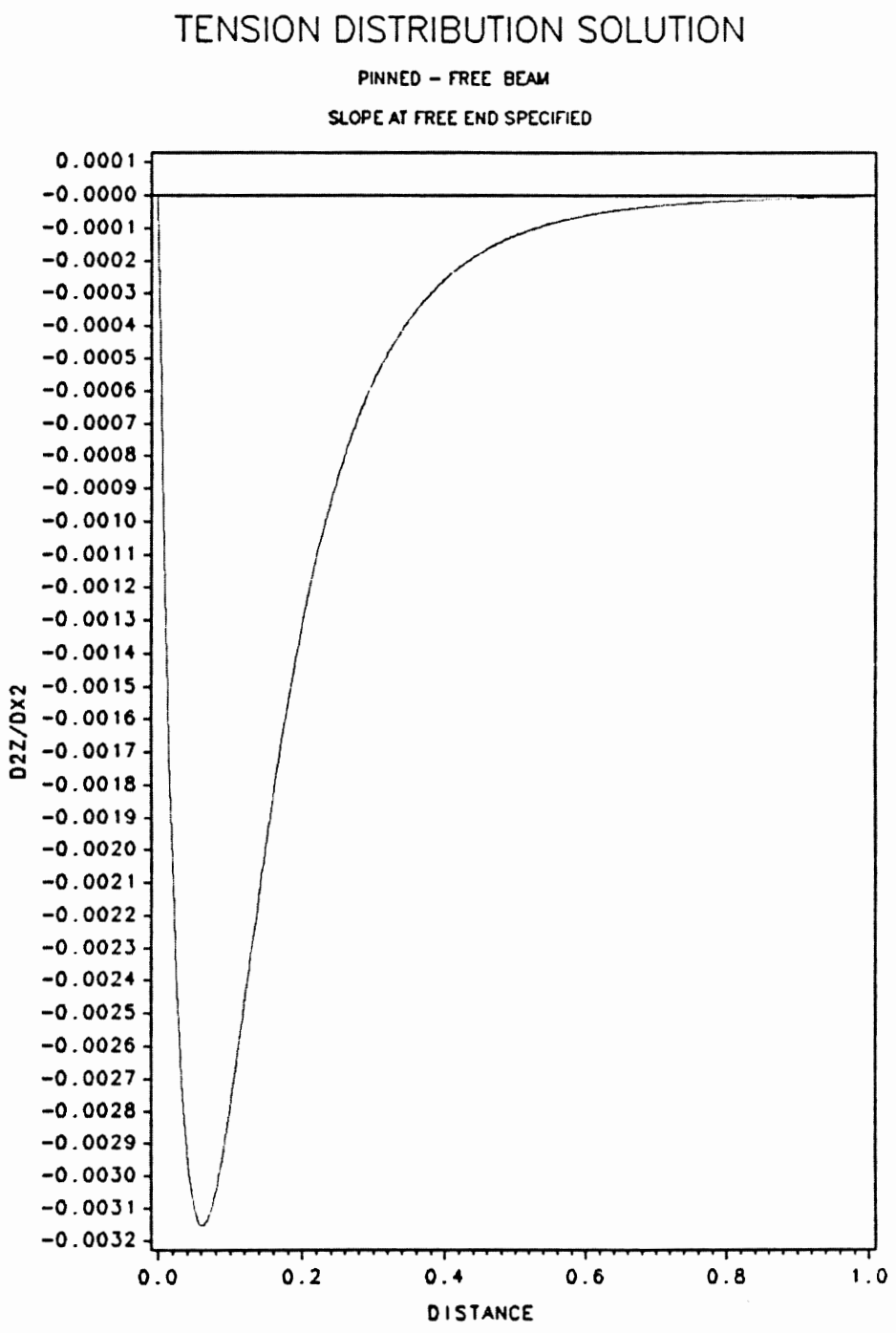

Figure 23 $\frac{\partial^2 \zeta}{\partial \varepsilon^2}$; Beam Model (back)

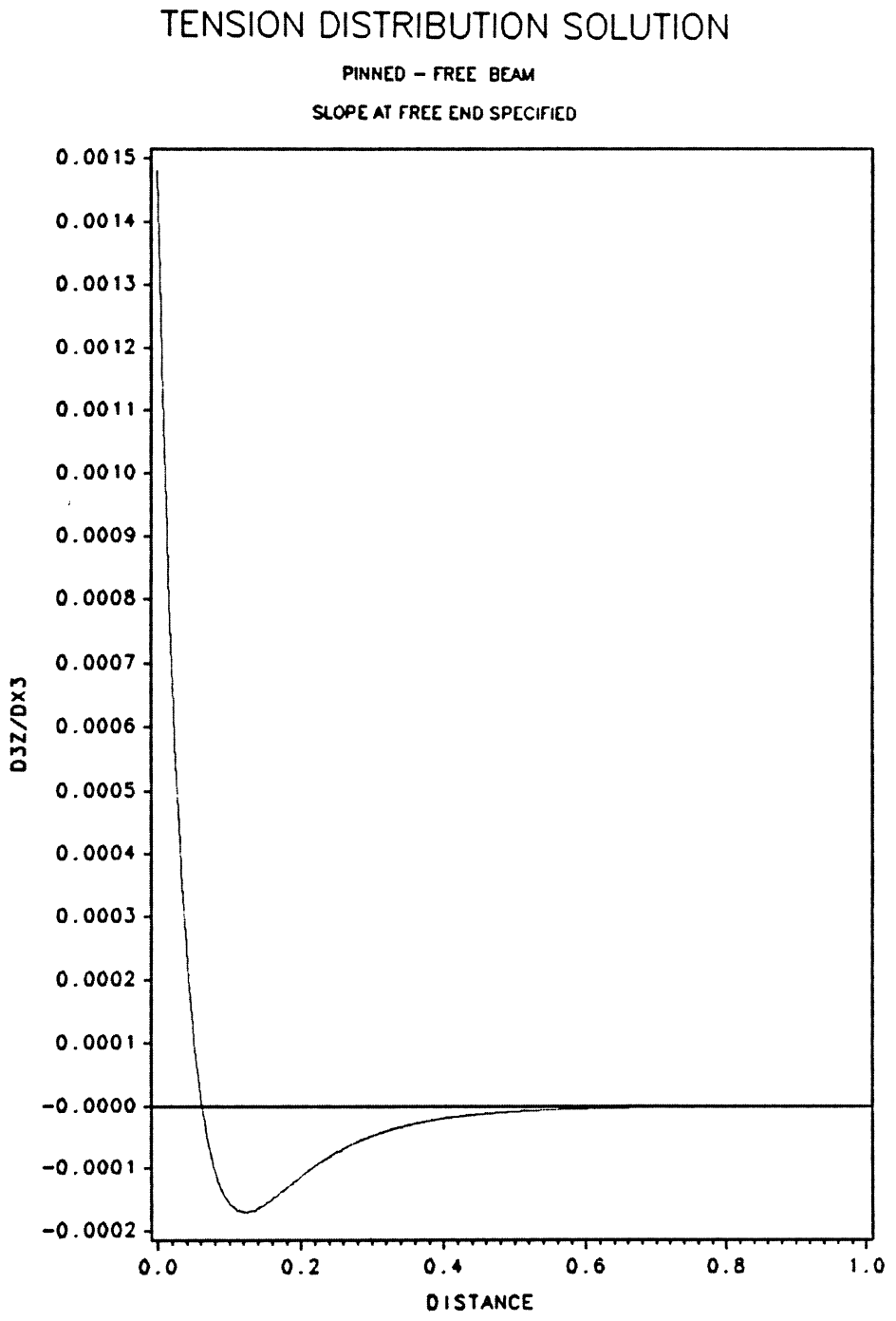

Figure 24 $\frac{\partial^3 \zeta}{\partial \varepsilon^3}$; Beam Model (back)

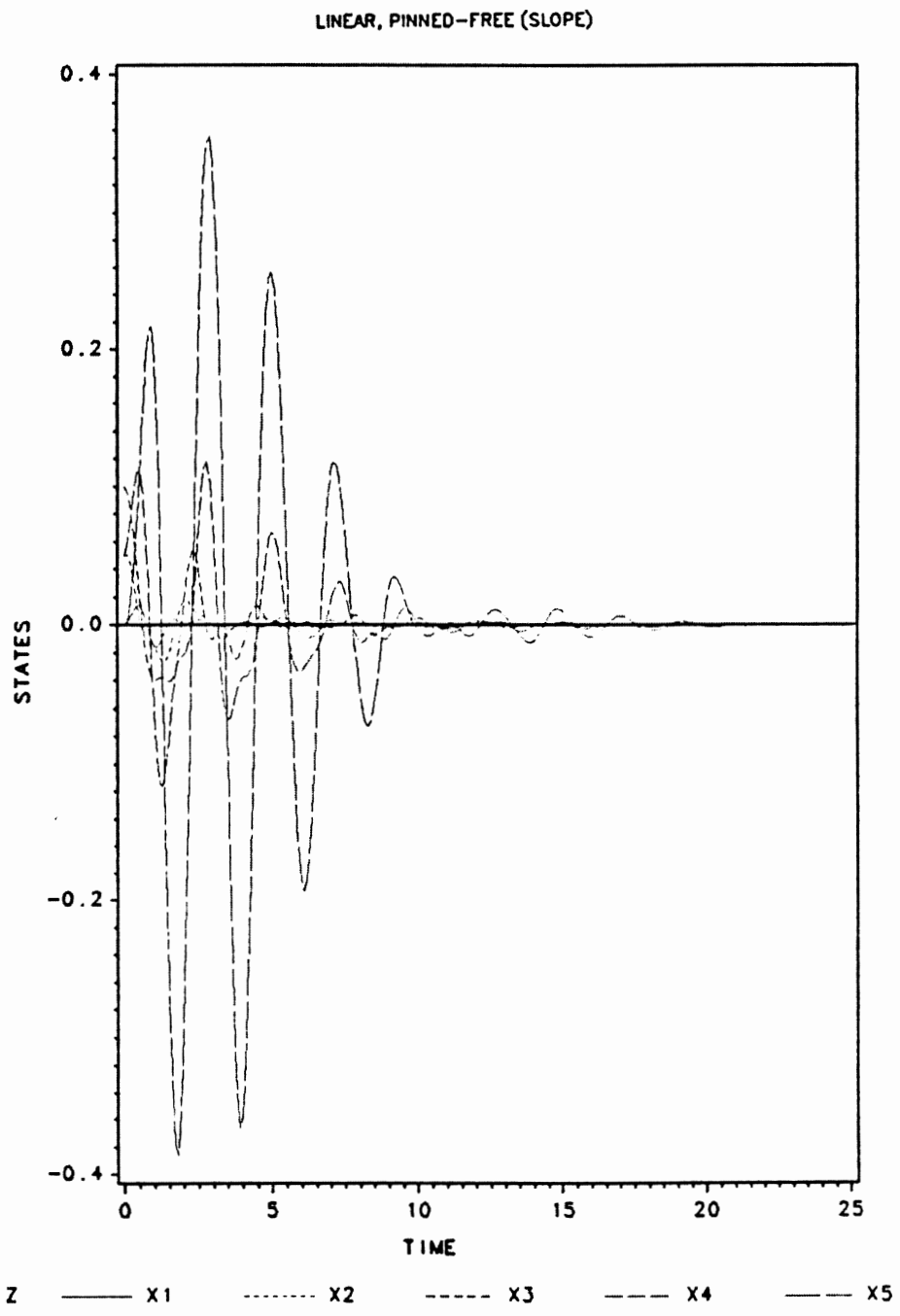

Figure 25 Hose Position; Linear Tension Model

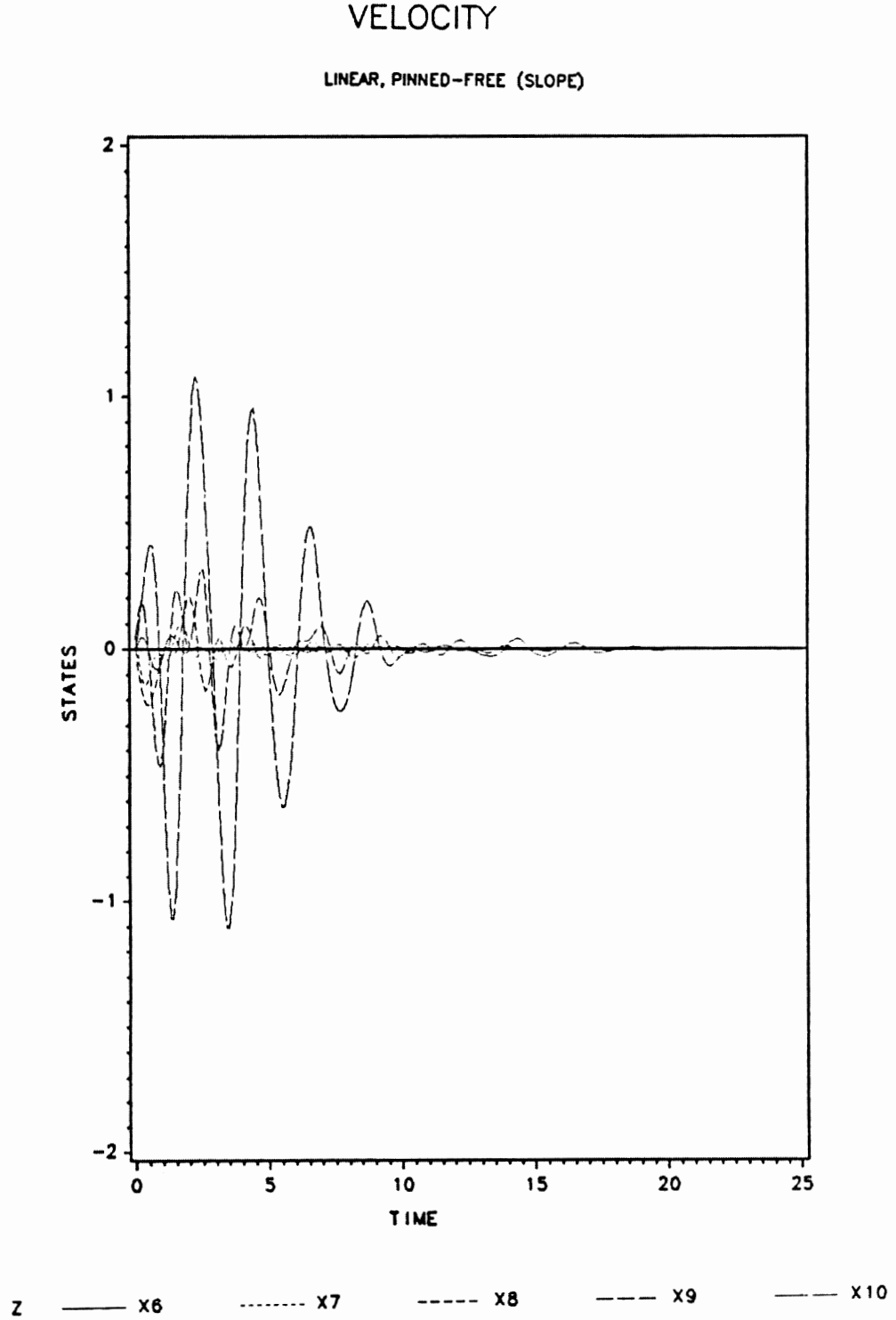

Figure 26 Hose Velocity; Linear Tension Model

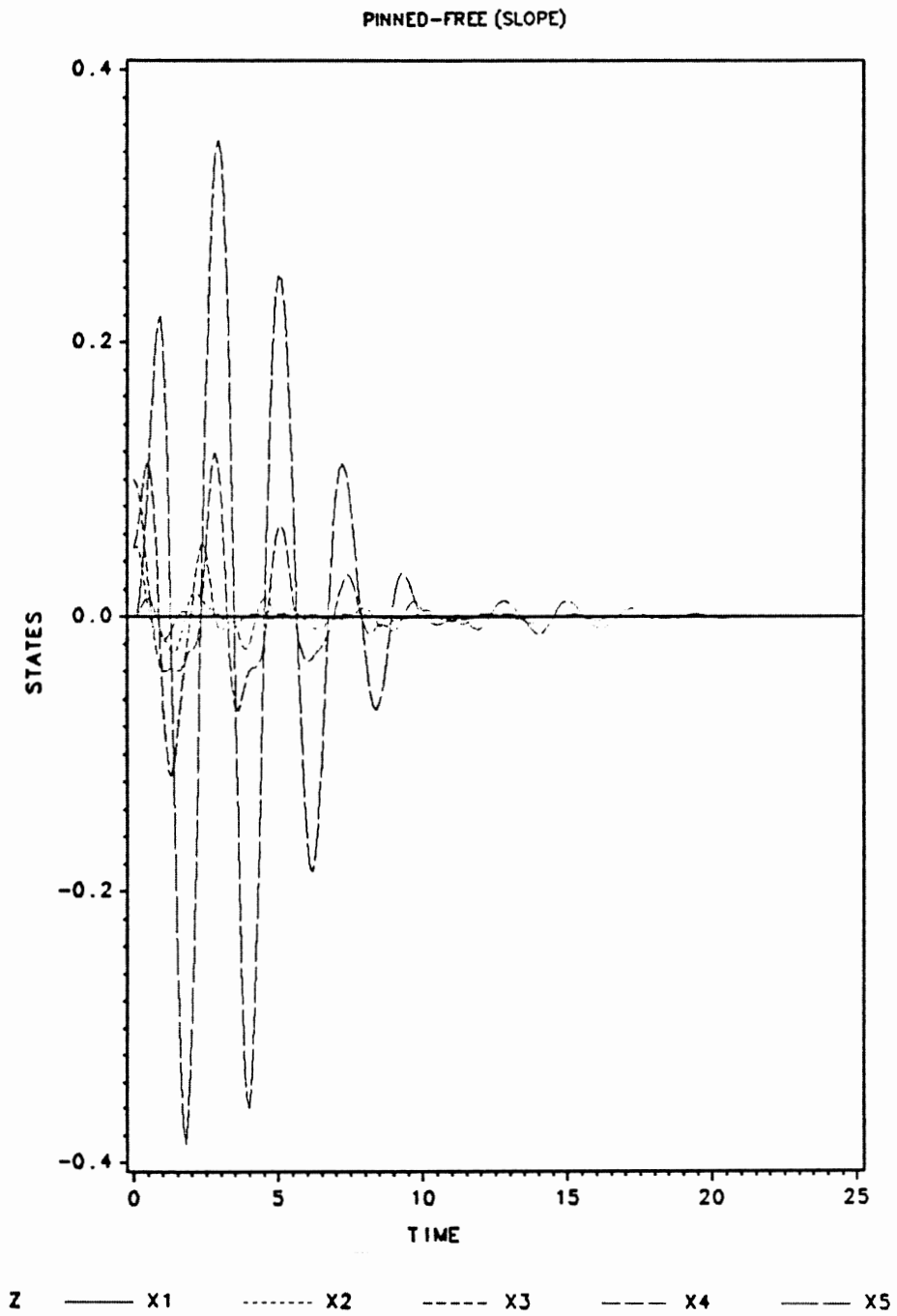

Figure 27 Hose Position; Beam Tension Model

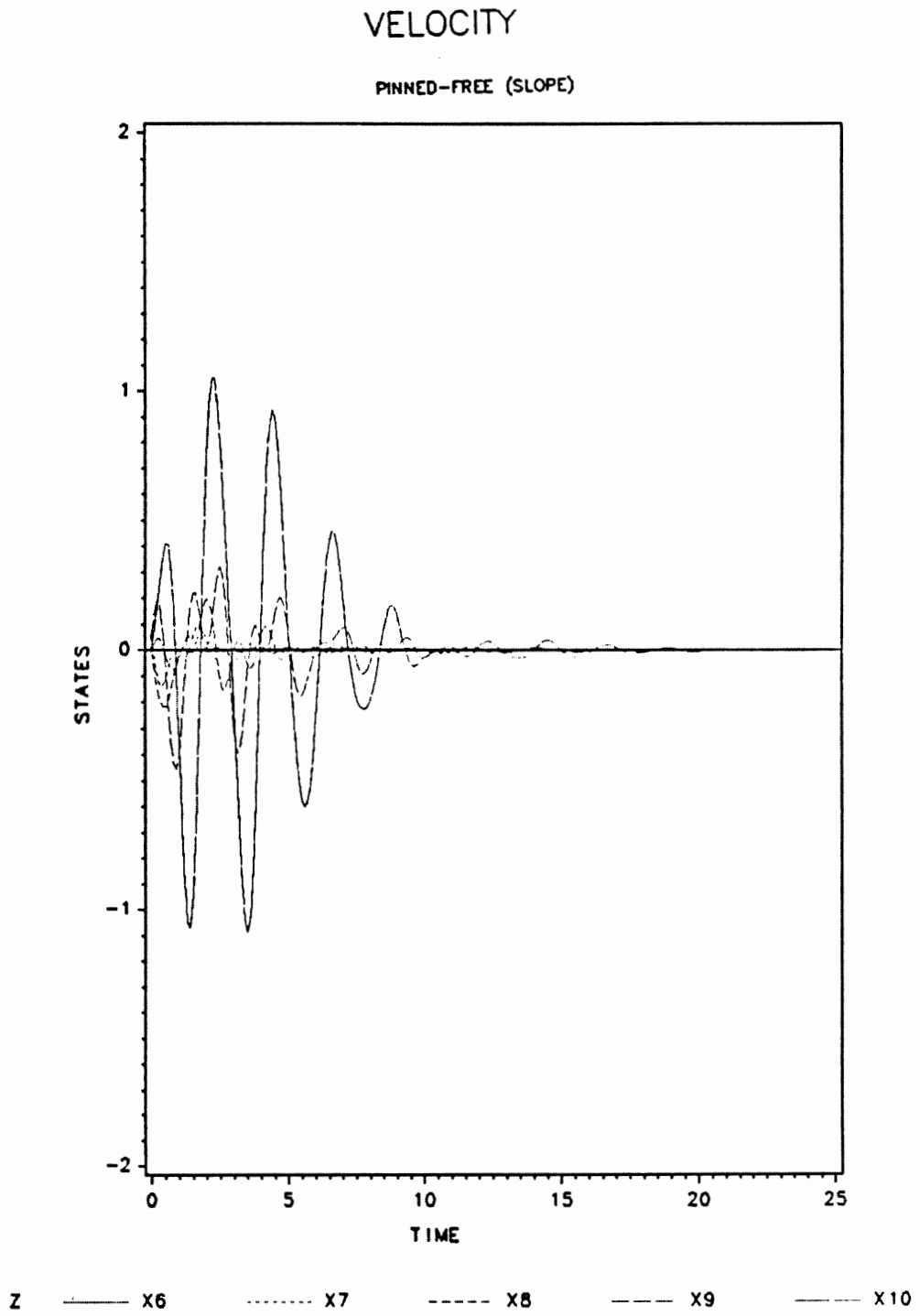

Figure 28 Hose Velocity; Beam Tension Model

The vita has been removed
from the scanned document